A new phenotyping pipeline reveals three types of lateral roots and a random branching pattern in two cereals

Sixtine Passot, Beatriz Moreno-Ortega, Daniel Moukouanga, Crispulo Balsera, Soazig Guyomarc'H, Mikael Lucas, Guillaume Lobet, Laurent Laplaze, Bertrand Muller, Yann Guédon

Short title

Lateral roots types revealed in two cereals

Corresponding author(s) details

Bertrand Muller, LEPSE, INRA, Montpellier SupAgro, Université de Montpellier, Montpellier, France

bertrand.muller@inra.fr

Yann Guédon, CIRAD, AGAP, Université de Montpellier, Montpellier, France

yann.guedon@cirad.fr

Title

A new phenotyping pipeline reveals three types of lateral roots and a random branching pattern in two cereals

All author names and affiliations

Sixtine Passot[1], Beatriz Moreno-Ortega[1], Daniel Moukouanga, Crispulo Balsera, Soazig Guyomarc'h, Mikael Lucas, Guillaume Lobet, Laurent Laplaze, Bertrand Muller[*], Yann Guédon[*]

[1]These authors contributed equally to the article.

IRD, DIADE, Université de Montpellier, Montpellier, France (S.P., D.M., M.L., L.L.)

CIRAD, AGAP, Université de Montpellier, Montpellier, France (S.P., B.M.-O., Y.G.)

INRA, LEPSE, Montpellier SupAgro, Université de Montpellier, Montpellier, France (B.M.-O., C.B., B.M.)

Laboratoire Mixte International Adaptation des Plantes et Microorganismes Associés aux Stress Environnementaux, Dakar, Sénégal (M.L., L.L.)

Université de Montpellier, DIADE, Montpellier, France (S.G.)

Agrosphere - IBG-3 Forschungszentrum Juelich, Germany and Earth and Life Institute, Université Catholique de Louvain, Belgium (G.L.)

[*]To whom correspondence should be addressed.

One sentence summary

Lateral roots in both pearl millet and maize can be categorized into three types based on growth rate profiles.

Author contributions

S.P. contributed to design, ran the pearl millet experiments, analyzed the data and wrote the manuscript; B.M.-O. contributed to design, ran the maize experiments, analyzed the data and wrote the manuscript; D.M. performed histological sections for pearl millet and maize and contributed to the pearl millet experiment; C.B. manufactured the rhizotrons and contributed to experiments; S.G. and M.L. contributed to pearl millet experiments; G.L. updated SmartRoot and added specific functions for this study; L.L. contributed to the design of the study and wrote the manuscript; B.M. designed the study and wrote the manuscript; Y.G. designed and implemented the statistical models, analyzed the data and wrote the manuscript.

This work was partly funded by the EURoot project (FP7-KBBE-2011-5/289300) and the NewPearl project in the frame of the CERES initiative (Agropolis Fondation AF 1301-015 as part of the "Investissement d'avenir" ANR-l0-LABX-0001-0l and Fondazione Cariplo FC 2013-0891). S.P PhD was funded by ENS Paris. B.M-O. PhD was partly funded by INRA (Environment & Agronomy division).

Present address: S.P: Earth and Life Institute, Université Catholique de Louvain, Belgium

Corresponding authors email:
bertrand.muller@inra.fr
yann.guedon@cirad.fr

Abstract

Recent progress in root phenotyping has focused mainly on increasing throughput for genetic studies while identifying root developmental patterns has been comparatively underexplored. We introduce a new phenotyping pipeline for producing high-quality spatio-temporal root system development data and identifying developmental patterns within these data. The SmartRoot image analysis system and temporal and spatial statistical models were applied to two cereals, pearl millet (*Pennisetum glaucum*) and maize (*Zea mays*). Semi-Markov switching linear models were used to cluster lateral roots based on their growth rate profiles. These models revealed three types of lateral roots with similar characteristics in both species. The first type corresponds to fast and accelerating roots, the second to rapidly arrested roots, and the third to an intermediate type where roots cease elongation after a few days. These types of lateral roots were retrieved in different proportions in a maize mutant affected in auxin signaling, while the first most vigorous type was absent in maize plants exposed to severe shading. Moreover, the classification of growth rate profiles was mirrored by a ranking of anatomical traits in pearl millet. Potential dependencies in the succession of lateral root types along the primary root were then analyzed using variable-order Markov chains. The lateral root type was not influenced by the shootward neighbor root type or by the distance from this root. This random branching pattern of primary roots was remarkably conserved, despite the high variability of root systems in both species. Our phenotyping pipeline opens the door to exploring the genetic variability of lateral root developmental patterns.

Introduction

Plant breeding has long ignored the belowground part of the plant but it is now acknowledged that the root system represents an opportunity for improving plant efficiency and tolerance to abiotic stresses (Bishopp and Lynch, 2015). A better knowledge of root system structure and function is thus needed for root system oriented crop improvement. Phenotyping, as the evaluation of heritable plant traits in a given environment and in a reproducible manner, is one key approach to extend this knowledge. Recent progresses in plant phenotyping platforms, including plant handling automation and computer assisted data acquisition, have allowed an increase in phenotyping throughput (i.e. the number of plants analyzed; Fahlgren et al., 2015b) which is critical for association studies and gene discovery. Besides increasing throughput, another strategy chosen in some phenotyping platforms is to improve data dimensionality and structure (Dhondt et al., 2013). In these platforms, the amount of data collected on a single plant is increased, either by measuring several traits that can be of different natures or by measuring the same trait at successive time points to focus on physiological processes (Fahlgren et al., 2015a).

The phenotyping of root systems presents specific challenges compared to the phenotyping of aerial parts of plants. The root system is by nature hidden and root phenotyping platforms have to make a compromise between the relevance of growth conditions and trait measurement feasibility. Most root phenotyping platforms focus on measurements at high throughput of selected root traits on a large number of plants, with the objective of detecting quantitative trait loci (QTL) usable in breeding (Kuijken et al., 2015). For example, Atkinson et al. (2015) reported a phenotyping platform where root systems grow in 2D on a filter paper for a few days. Platforms where root systems grow in 3D have also been developed (Iyer-Pascuzzi et al., 2010) and used for QTL detection (Topp et al., 2013). Most of these platforms generate traits that give a global view of the root architecture. By contrast, the development of individual roots during long periods of time is rarely studied, whereas temporal analyses are more developed for the aerial parts (see e.g. Lièvre et al., 2016). These studies have been hampered by the difficulty of collecting individual root growth data.

In addition, the analysis of structured data such as root growth rate profiles is more challenging than the analysis of simple root traits.

The variability of lateral root length along a primary root is a widely observed feature of root systems (reviewed by Forde (2009)), having been reported for annual dicots (e.g. sunflower (*Helianthus annus*), Aguirrezabal et al., 1994), annual monocots (e.g. maize (*Zea mays*), Jordan et al., 1993; Varney et al., 1991; Wu et al., 2016), and perennials (oak (*Quercus robur*), Pagès, 1995; rubber tree (*Hevea brasiliensis*), Thaler and Pagès, 1996; banana (*Musa acuminata*), Lecompte et al., 2005). It has also been observed in the model species Arabidopsis (*Arabidopsis thaliana*) (Freixes et al., 2002). Although variability in length likely originates from variability in growth rate, most of these descriptions do not consider growth dynamically. When they do (Pagès, 1995; Thaler and Pagès, 1996), they generally consider that the variability of growth rate profiles forms a continuum but do not investigate a possible structuring into distinct classes. Nevertheless, different lateral root types have been described, in particular in cereals, but these classifications are based on anatomical traits or diameter. Accordingly, three to four lateral root types have been reported in maize (Varney et al., 1991), three in pearl millet (*Pennisetum glaucum*) (Passot et al., 2016) and rice (*Oryza sativa*) (Gowda et al., 2011; Henry et al., 2016), and five in wheat (*Triticum aestivum*), barley (*Hordeum vulgare*), and triticale (*Triticale hexaploide*) (Watt et al., 2008).

The variability of lateral root growth is likely an important lever of root system efficiency (Forde, 2009; Pagès, 2011). In order to provide an efficient frame to study this phenomenon and to characterize genetic and/or environmental impacts on that variability, we designed a phenotyping pipeline for producing high-quality spatio-temporal root system development data with a focus on lateral roots. This pipeline combines the SmartRoot image analysis system (Lobet et al., 2011), which is able to reconstruct consistent spatio-temporal data on the basis of successive snapshots of root system architecture, with temporal and spatial statistical models. We used it to characterize the early developmental patterns of root systems in two cereals, pearl millet and maize. In a first step, lateral root growth rate profiles were analyzed using semi-Markov switching linear models; see Lièvre et al. (2016) for another application

of similar statistical models. This model-based clustering of growth rate profiles led us to identify three types of lateral root. We also applied this clustering approach to the *rootless concerning crown and seminal roots* (*rtcs*) maize mutant affected in auxin signaling and to maize plants exposed to severe shading. We then investigated the relationships between lateral root types and morphological (apical diameter profile in maize) and anatomical (stele diameter and central xylem tracheary element diameter in pearl millet) traits. In a second step, potential dependencies in the succession of lateral root types along the primary root were analyzed using variable-order Markov chains leading to a precise characterization of the primary root branching pattern. Our phenotyping pipeline opens the door to a quantitative, model-assisted characterization of developmental patterns of lateral roots to support root system oriented crop improvement.

Results

Daily images of growing root systems were recorded for 15 and 21 days in a rhizotron system to analyze early root system development and architecture, in pearl millet and maize respectively. These temporal limits were imposed by the root systems reaching the bottom of the rhizotron. The difference between the two species was a consequence of a higher average elongation rate in pearl millet compared to maize. The ability of SmartRoot (Lobet et al., 2011) to cross-link information corresponding to different time points was then used to build consistent spatio-temporal data of root system development and architecture on the basis of the corresponding series of images. We chose to decompose the analysis of these spatio-temporal data into two steps:

1. *temporal analysis*: we first analyzed growth rate profiles of lateral roots using semi-Markov switching linear models. Lateral roots were classified into types as a byproduct of this longitudinal data analysis.
2. *spatial analysis*: The intervals between consecutive lateral roots and the succession of lateral root types along the primary root were then analyzed.

A model-based clustering of lateral root growth rate profiles reveals three classes of lateral root in pearl millet and maize

The dataset was composed of growth rate profiles of 1254 lateral roots from 8 plants in pearl millet and of 3050 lateral roots from 13 plants in maize. The exploratory analysis of these growth rate profiles highlighted a strong longitudinal organization with growth rates either increasing or decreasing with lateral root age (Fig. 1). The growth rate profiles are essentially divergent after root emergence and the growth rate dispersion increases with the root age. Hence, lateral roots can be roughly ordered according to their growth rate profiles. This raised the question of a stronger structuring of these longitudinal data beyond a simple ordering of lateral root growth rate profiles. We thus chose to investigate a model-based clustering of these longitudinal data. This raised two types of difficulties: (i) the growth rate profiles were short and highly variable among lateral roots (1 to 10 and 1 to 17 successive growth rates for pearl millet and maize, respectively) and (ii) a high proportion of lateral roots were still growing the last date of measurement. We thus designed a statistical model for clustering growth rate profiles, using only profiles lasting at least 5 days, based on the following assumptions: (i) a growth rate profile is modeled by a single growth phase either censored (to take into account lateral roots still growing the last date of measurement) or followed by a growth arrest and (ii) changes in growth rate within a growth phase are modeled by a linear trend. This strong parametric assumption is a consequence of the short length of growth rate profiles. Hence, linear trend models should be viewed as instrumental models for clustering growth rate profiles and not as models for fitting accurately each growth rate profile.

The proposed statistical model is composed of growth states, each corresponding to a lateral root growth rate profile type. A distribution representing the growth phase duration (in days) and a linear model representing changes in growth rate during the growth phase are associated with each of these growth states. Growth states are systematically followed by a growth arrest state. The overall model is referred to as a semi-Markov switching linear model (SMS-LM; see Materials and Methods and Supplemental Methods S1 for a formal definition and Fig. 2 and Supplemental Fig. S1 for pearl millet and maize SMS-LMs, respectively). The number of states of a SMS-LM is thus the number of lateral root types plus one (the single growth arrest state). This kind of integrative statistical model makes it possible to estimate growth phase duration distributions combining complete and censored growth phases. The

mechanism associated with a SMS-LM can be described as follows: A growth state is randomly selected according to an initial distribution. This initial distribution represents the lateral root type proportions. A growth phase duration is then randomly selected according to the corresponding distribution of the selected growth state. The growth rate then changes with time according to the linear trend model associated with the selected growth state until the end of the growth phase and the transition to the growth arrest state. In such SMS-LM, the transitions from the growth arrest state to a growth state are not possible and each state can be visited at most once (see illustration in Fig. 2 and Supplemental Fig. S1).

We next had to select the number of growth states (i.e. the number of lateral root types). Because of the specific structure of the model where each state can be visited at most once, the usual model selection criteria such as the Bayesian information criterion do not apply. We thus designed an empirical model selection method for selecting the number of growth states which is detailed in Supplemental Methods S2 and illustrated by Supplemental Tables S1 and S2 for pearl millet and maize, respectively. We selected for both species three lateral root types that correspond to the best compromise between (i) the proportion of unambiguously assigned lateral roots (between-cluster criterion) and (ii) the relative dispersion of growth rate profiles particularly for the most vigorous root type (within-cluster criterion). Having two classes only would dramatically increase the dispersion for the most vigorous root type (Supplemental Fig. S2 for pearl millet) whereas having four classes would increase the proportion of ambiguously assigned roots (Supplemental Fig. S3). Hence, clustering of lateral roots based on their growth rate profiles revealed three lateral root types in both pearl millet and maize. These three types ordered in decreasing vigor will be referred to as A, B and C.

Growth phases are similar in both species

The estimated growth phase duration distributions are similar for each lateral root type between pearl millet and maize (Table 1; Fig. 3). The censoring level is defined as the proportion of growth phase incompletely observed for a given lateral root type (the corresponding lateral roots were still growing the last date of measurement). The censoring level is high for type A, intermediate for type B and rather low for type C

(Table 1). The higher censoring level for pearl millet compared to maize is a direct consequence of the shorter average growth rate profiles for pearl millet (in relation to the faster root growth in this species) since the growth phase duration distributions are similar for the two species. It should be noted that the length of the growth rate profiles (i.e. the number of successive growth rates) are similar for the different lateral root types of a given species (Supplemental Fig. S4) suggesting no preferential location of the lateral roots of the different types along the primary root.

Comparison of growth rate profiles between the two species

Only growth rate profiles of length ≥ 5 (corresponding to 652 lateral roots of cumulative length 4367 for pearl millet and 2029 lateral roots of cumulative length 17257 for maize) were used for the building of SMS-LMs. Once a SMS-LM was built, the growth rate profiles belonging to the learning sample were assigned to lateral root types (see Fig. 1A for examples of clustering of lateral roots in pearl millet and Fig. 1B for examples of clustering of lateral roots in maize). The posterior probabilities of the optimal assignment of growth rate profiles of length ≥ 5 to lateral root types (i.e. weights of the optimal assignment among all the possible assignments) were most often high − 92% above 0.8 and 88% above 0.9 for pearl millet (Supplemental Fig. S3A) and 94% above 0.8 and 81% above 0.8 for maize (Supplemental Fig. S3B) − indicating a clear between-cluster separation; see Supplemental Methods S2. Growth rate profiles of length < 5 (test sample corresponding to 602 lateral roots of cumulative length 1945 for pearl millet and 1021 lateral roots of cumulative length 2958 for maize) were also assigned to lateral root types using the previously estimated SMS-LM. The posterior probabilities of the optimal assignment of these growth rate profiles to lateral root types were most often high despite the limited information conveyed by these profiles: 83% above 0.8 and 73% above 0.9 for pearl millet (Supplemental Fig. S5A) and, 85% above 0.8 and 68% above 0.9 for maize (Supplemental Fig. S5B). These independent assignments constitute clear elements of validation of the clustering assumption. In order to assess the separation of lateral root types during growth, we compared the classification accuracy between growth rate profiles (whatever their length) truncated at successive lengths. Growth rate profiles truncated at length 1, 2, 3 and 5, and untruncated growth rate profiles were assigned to lateral root types (Fig. 4). The posterior probabilities of the optimal assignment of truncated growth rate profiles

show that the classification accuracy improves rapidly the very first days of growth before stabilizing around day 5 consistently with the divergence of growth rate profiles after root emergence (Fig. 1). In both species, daily median growth rates (computed from all the growth rate profiles whatever their length) are divergent between the three types of lateral roots (Fig. 5 A,B). Type A median growth rate stays positive at all ages in both species. Type B median growth rate reaches zero at day 8 in pearl millet and at day 6 in maize while type C median growth rate reaches zero at day 3 in both species. The main differences between the two species, apart from differences in growth rates, concern (i) type A lateral roots for which median growth rate continues to increase in pearl millet whereas it stays nearly constant after a few days in maize and (ii) type B lateral roots for which median growth rate stays nearly constant up to day 5 in pearl millet whereas it starts to decrease immediately after emergence in maize. Dispersions in growth rate profiles are rather similar between the two species for types B and C; see the mean absolute deviation profiles in Fig. 5 A,B. A regular increase in mean absolute deviation with root age can be observed for type A lateral roots in maize. This may be due to the mixing at the later ages within this class of lateral roots whose growth rate started to decrease with lateral roots whose growth rate continued to increase.

The apical diameter profiles partially match the different root types identified in maize

The optimal assignment of lateral roots to types computed using the estimated SMS-LM was used to analyze the link between growth rate types and root apical diameter in maize (the lower apical diameter of lateral roots combined with the image resolution did not allow this analysis in pearl millet). Apical diameter profiles (Fig. 5C) clearly distinguish type A (higher diameters) from type B and C lateral roots but not type B from type C lateral roots (see the overlaps between apical diameter distributions for the successive ages in Supplemental Table S3). Apical diameter gradually decreases with root age for types B and C and converges towards median apical diameter around 230 µm. This corresponds to a high proportion of arrested roots and suggests the occurrence of a threshold value for the apical diameter, below which roots will ultimately stop growing.

Linking lateral root growth rate profile with anatomy in pearl millet

Previous studies have shown that different lateral root types can be defined based on their anatomy in pearl millet (Passot et al., 2016). To explore the links between root growth and root anatomy, we observed cross sections in 35 pearl millet lateral roots with contrasting growth rate profiles. Lateral roots were assigned to one of the three types previously defined, based on their growth rate profile. Stele diameter and central xylem tracheary element (XTE) diameter, previously shown to be contrasting among individual roots in pearl millet (Passot et al., 2016) were measured. The classification of growth rate profiles in types A, B and C is mirrored by a ranking of both stele diameter and central XTE diameter, although there is some overlap between types (Fig. 6). This is confirmed by the high Spearman's rank correlation coefficients between anatomical traits and lateral root types for pearl millet ($\rho = 0.81$ between stele diameter and lateral root types and $\rho = 0.91$ between central XTE diameter and lateral root types).

The definition of lateral root types is neither affected by a mutation altering auxin signaling nor by a shading treatment in maize

One of the aims of this study was to provide a pipeline of analysis able to account for genetic and environmental effects. We thus analyzed the growth rate profiles of lateral roots of a maize mutant with altered auxin signaling (*rtcs* mutant; *RTCS* encodes a LOB-domain transcription factor and carries auxin-responsive elements in its promoter; Taramino et al., 2007) and of wild-type maize plants exposed to severe shading. The datasets were composed of growth rate profiles of 1597 lateral roots from 9 *rtcs* mutant plants, and of 572 lateral roots from 6 shaded plants. Growth rate profiles of 994 lateral roots of length ≥ 5 (length up to 14 and cumulative length of 7022) were used for the building of SMS-LMs for the *rtcs* mutant. Growth rate profiles of 540 lateral roots of length ≥ 5 (length up to 12 and cumulative length of 4129) were used for the building of SMS-LMs for shaded plants. Applying the empirical model selection procedure previously described, we obtained three lateral root types for the *rtcs* mutant and two for the shaded plants corresponding to types B and C identified in unshaded wild-type plants. The posterior probabilities of the optimal assignment of growth rate profiles of length ≥ 5 to lateral root types, using the SMS-LMs previously estimated on the basis of these learning samples, were most often high $-$ 91% above

0.8 and 87% above 0.9 for the *rtcs* mutant, and 93% above 0.8 and 80% above 0.9 for the shaded plants − indicating a clear between-cluster separation. Growth rate profiles of length < 5 (test sample corresponding to 603 lateral roots of cumulative length 1499) were also assigned to lateral root types using the SMS-LM previously estimated for the *rtcs* mutant. The posterior probabilities of the optimal assignment of these growth rate profiles to lateral root types were most often high despite the limited information conveyed by these profiles: 85% above 0.8 and 50% above 0.9. These independent assignments constitute clear elements of validation of the clustering assumption for the *rtcs* mutant. The results of independent assignments are not reported for the shaded plants since there were only 32 growth rate profiles of length < 5 in this case. Both for the *rtcs* mutant and the shaded plants, the growth rate profiles were assigned to lateral root types using both the SMS-LM built on the basis of these lateral roots and the SMS-LM built on the basis of the unshaded wild-type plants. We obtained a match of 94% (938 lateral roots among 994) between the two independent assignments for the *rtcs* mutant and a match of 91% (492 lateral roots among 540) for the shaded plants indicating that the lateral root types are robustly defined. The estimated growth phase duration distributions are similar for each lateral root type between the *rtcs* mutant and the wild-type SMS-LM as well as between the shaded and the unshaded SMS-LM for types B and C (Fig. 7, Table 1). The median growth rate profiles are only slightly affected by the mutation and shading treatment (Fig. 8A, Supplemental Figs. S6 and S7). In summary, the definition of lateral root types remains robust irrespective of the genotype or the environmental treatment. Differences with the control wild type concerned (i) the absence of type A lateral roots for the shaded plants, (ii) the higher proportion of type B lateral roots compensated by a lower proportion of type C lateral roots for the *rtcs* mutant and a higher proportion of type C lateral roots for the shaded plants (Table 2). Results concerning the shaded plants are consistent with the expectation of an inhibition of root growth in relation with a restriction in the supply of carbohydrates. Moreover, we could observe (iii) larger diameters compared to wild type for all root types in the *rtcs* mutant and for type C in the shaded plants (Fig. 8B) and (iv) a hierarchy in apical diameter profiles between types B and C for the *rtcs* mutant whereas type B and C apical diameter profiles are confounded in both wild-type and shaded plants (see Fig. 8B and Supplemental Table S3).

Identification of a stationary random primary root branching pattern

In order to characterize the primary root branching pattern in both pearl millet and maize, we first analyzed the length of the intervals between consecutive lateral roots and then, the potential dependencies between successive lateral root types (A, B and C) along the primary root. We first evaluated the impact of the root type on the length of the interval between a lateral root and its nearest neighbor in the rootward direction. No difference was found between the mean interval length for the three root types in both species (ANOVA, *p*-value = 0.83 and 0.33 for pearl millet and maize, respectively; see Table 3). The same type of analysis was conducted splitting intervals into 9 groups, depending on the types of the two lateral roots delimiting the interval (Supplemental Tables S4 and S5 for pearl millet and maize, respectively). No effect of the lateral root types was found on the interval lengths (ANOVA, *p*-value = 0.52 and 0.15 for pearl millet and maize, respectively). Hence, there is no influence of the root types on the length of the interval between two consecutive lateral roots.

We then analyzed the potential dependencies within lateral root type sequences ignoring the length of the intervals between consecutive lateral roots (the branching sequences from the collar rootward were thus simply indexed by the rank of the successive lateral roots along the primary root). We first computed the Spearman rank autocorrelation function for these sequences (the lateral root type can be considered as a categorical ordinal variable with the three possible ordered categories A, B and C). This autocorrelation function measures the correlation between ordinal variables at different distances apart. The autocorrelation function for positive lags is within the confidence interval corresponding to the randomness assumption for most of the plants (Supplemental Fig. S8 A-D), indicating that the distribution of the lateral root types along the primary root was stationary and suggesting no marked dependencies between successive lateral root types. This finding is consistent with the similar frequency distributions of the length of growth rate profiles for the three lateral root types (Supplemental Fig. S4). Since the length of a growth rate profile directly depends on the time of emergence of the lateral root and is thus related to its position along the primary root, this suggests that the proportions of the three lateral root types along the

primary roots were roughly stationary. For some individuals (one for pearl millet and 4 for maize), the autocorrelation function fluctuates around the positive confidence limit (Supplemental Fig. S8 E,F) indicating a slight non-stationarity. We further investigated primary root branching sequences applying a statistical modeling approach. To this end, we modeled potential dependencies between successive lateral root types along the primary roots. Three-state variable-order Markov chains, each state corresponding to a lateral root type, were built. The memories of variable-order Markov chains were selected (Csiszár and Talata, 2006) for each primary root branching sequence and for samples of branching sequences corresponding to each species. For all plants and for both species, a zero-order Markov chain was selected. This confirmed that the type of a lateral root was independent of the type of the previous lateral roots. Hence, our results indicate that there is no influence of the lateral root growth pattern on the distance to or on the growth pattern of the next lateral root in pearl millet and maize.

Inter-individual variability of the branching pattern

We evaluated the variability of the length of the interval between consecutive lateral roots and of the proportions of lateral root types among individual plants for each species. The mean interval lengths were not equal in all plants (ANOVA, $p < 10^{-5}$ for pearl millet and $p < 10^{-6}$ for maize). Plants were thus classified according to Tukey's honest significant difference test. Two overlapping groups were found, both for pearl millet and maize (Supplemental Fig. S9), with average interval length ranging from 0.21 to 0.31 cm in pearl millet, and from 0.14 to 0.25 cm in maize. Significant differences among plants were also found for lateral root type proportions both for pearl millet and maize (Kruskal-Wallis test, $p < 10^{-10}$ and $p < 10^{-15}$ respectively, Fig. 9). For pearl millet, the 8 plants were separated into three groups with two groups overlapping and the type A lateral root proportion ranging from 0.06 to 0.21. The 13 maize plants were separated into 6 groups, with some overlaps between groups and the type A lateral root proportion ranging from 0 to 0.2. These results indicate that both species show significant between-individual differences in terms of length of intervals between consecutive lateral roots and lateral root type proportions. These differences were neither related to plant biomass, seed biomass, nor to total root system length (results not shown). However, despite differences between

plants in terms of lateral root type proportions, the stationary random branching pattern is markedly conserved in all plants.

Discussion

A new longitudinal data analysis approach to identify lateral root types based on growth rate profiles

In this study, we designed a pipeline for analyzing lateral root growth rate profiles and primary root branching pattern and applied it to explore the diversity of lateral roots in two cereals, maize and pearl millet. Previous efforts to classify lateral roots in cereal species have been reported (Varney et al., 1991; Watt et al., 2008; Rebouillat et al., 2009; Henry et al., 2016; Passot et al., 2016) but these classifications were often based on anatomical traits, mainly root diameter and vasculature. A first difficulty comes from the fact that some morphological traits change along lateral roots, typically root diameter (Wu et al., 2016), which was confirmed in our maize data. A different classification method, based on growth rates, was reported in rice (Rebouillat et al., 2009) for which growth rates were highly contrasting among lateral roots but assignment to classes was based on expert knowledge. In oak, lateral roots were classified based on empirical thresholds applied to individual growth rates (Pagès, 1995). Here we assigned lateral roots to classes based on their growth rate profiles using dedicated statistical models. A strength of these statistical models is the capability to optimally combine complete and censored growth rate profiles since some lateral roots were still growing at the end of the experiment. Our approach revealed three similar types of lateral roots in two different cereal species. In previous studies, three anatomical types of lateral roots were identified in maize (Varney et al., 1991; Moreno-Ortega et al., 2017) and pearl millet (Passot et al., 2016) and our results in pearl millet confirm that these types are well related to the types obtained from our model-based clustering of growth rate profiles. In maize, the root apical diameter profiles were at least partly linked to growth rate profiles, confirming a behavior already seen in other species such as oak or rubber tree (Pagès, 1995; Thaler and Pagès, 1996) where diameter and growth rate change in parallel. Taken together, our results thus suggest that these changes observed at the macroscopic scale are at least partly linked to temporal changes in root anatomy and vasculature.

Variability between plants is known to be particularly high for root systems (Williamson et al., 2001; Ashehoug and Callaway, 2014) and this, in principle, hampers our capacity to identify patterns within a given architecture. Our classification was sufficiently robust to accommodate the high inter-individual variability among replicate plants within the same experimental set-up. We failed to identify the sources of such variability since neither seed mass, nor leaf area were able to account for differences among individuals in line with the idea that inter-individual variability could be an intrinsic property of root systems (Forde, 2009). Our classification was also sufficiently robust to accommodate genetic (mutation in auxin signaling) and environmental variation (severe shading) showing that these sources of variation translate into altered proportions of lateral root types, not into a redefinition of each type. The strong reduction of mean lateral root length upon shading was expected (Freixes et al., 2002; Muller et al., 1998) but our analysis revealed that this effect was the result of the complete disappearance of vigorous, fast growing lateral roots and a large increase in the proportion of lateral roots showing a rapid growth cessation. A mutation in auxin signaling which controls the formation of nodal roots (Hetz et al., 1996) only had a limited impact on the proportion of the three lateral root types whereas it had great impact on lateral root diameter. This suggests that our pipeline of analysis can be used to identify and characterize growth patterns within complex and variable architectures and to evaluate related functional hypotheses such as the impact of hormone signaling (De Smet et al., 2003; Lavenus et al., 2013) or carbohydrate availability (Bingham and Stevenson, 1993).

Origin and fate of the three lateral root types

The identification of three lateral root types raises questions about their origin during development. In rice, fast-growing lateral roots are also thicker and additional periclinal cell divisions in the endodermal cell layer producing additional mesodermal cell layers during the process of primordia establishment have been reported in these large lateral roots (Rebouillat et al., 2009). Variability in size of different lateral root primordia has been reported in maize (MacLeod, 1990) and could account for differences in apical diameter, at least at emergence. Accordingly, it has been proposed that lateral root variability would be determined early in development and would be

tightly associated with morphology and anatomy (Thaler and Pagès, 1996). The relationship between root anatomy (stele and central XTE diameter) and types based on growth rate profile, evidenced in pearl millet, goes in this direction. In maize, lateral root types could also be well defined based on stele and vessel diameters (Varmey et al., 1991) and it will be necessary to explore the match between anatomy and growth patterns in this species. Root diameters at emergence are also ranked according to growth rate profiles in maize but this ranking is not strict as shown by the large overlap of apical diameters between lateral root types. Another possibility is that growth rate variability would be determined after emergence in order to adapt in a more plastic manner to the local environmental conditions the roots encounter. Such plasticity is commonplace in root systems and lateral roots are the most dynamic place for this plasticity (Drew, 1975; Farrar and Jones 1986). The parallel between apical root diameter profiles and growth rate profiles in maize is also in favor of a progressive assignment of roots into one of the three types. These two hypotheses may not be exclusive and growth patterns may result from a combination of these two influences that would occur pre- and post-emergence. Factors influencing initial growth rate, growth maintenance and growth arrest could also be different, therefore rendering the picture more complex and leading to developmental patterns of lateral roots globally more plastic to face a variability of external and internal clues (Malamy, 2005). Interestingly, we showed recently that the typology of growth patterns found in the present study, matches a typology of meristem length being far longer in type A lateral roots compared to type B lateral roots (mean of 450 µm and 280 µm, respectively) and lacking in type C lateral roots (Moreno-Ortega et al., 2017). Moreover, meristem length variation was associated with a variation of the length of the elongation zone suggesting that growth variation is the result of coordinated variations in both cell production and cell expansion (Moreno-Ortega et al., 2017).

Which role for the three lateral root types?

The sharing of tasks between the three lateral root types could contribute to the overall root system efficiency in front of a changing and unpredictable environment. In maize, short roots (i.e. type C roots) with xylem differentiated down to the tip are suspected to facilitate water uptake (Varney and McCully, 1991; Wang et al., 1994). In rice, the presence of short, thin and abundant lateral roots has been interpreted functionally as

543 ‘super root hairs’ (Nestler et al., 2016), increasing the root surface area and nutrient
544 uptake, in particular for immobile ions such as phosphorus (P) while at the same time
545 having a low carbon cost as compared to long lateral roots. By contrast, long lateral
546 roots (i.e. type A roots) may contribute to widen the exploration in the horizontal
547 dimension beyond the limited horizon explored by nodal roots in opposition to
548 exploration in depth covered by the primary root. They also contribute to the build-up
549 of the overall root architecture since only long lateral roots participate in higher levels
550 of branching (Gowda et al., 2011). In perennials, only long lateral roots contribute to
551 the perennial structure of the plant (Coutts, 1987). The functional efficiency of the root
552 system may also be linked to the proportions of these different lateral root types. The
553 production of too many long lateral roots is likely counterproductive because of their
554 carbon cost, as well as competition among individual roots for the capture of mobile
555 soil resources such as water or nitrate (Lynch, 2018). Finally, the plasticity of the
556 proportions of these different lateral root types could also contribute to the efficiency
557 of the root system. In rice, the proportions of short and long lateral root are highly
558 plastic in response to low P and there exists some genetic variability of this plasticity
559 (Vejchasarn et al 2016). The role of type B lateral roots is more speculative but they
560 could constitute a trade-off between the two opposite strategies of type A and C lateral
561 roots. They could also constitute a pool of potentially fast growing roots if conditions
562 are favorable. The added value of this overall variability and plasticity to enhance root
563 foraging capacity was already suggested (Forde, 2009) while its cost/benefit advantage
564 compared to more homogenous lateral root patterns was demonstrated using simulated
565 root systems (Pagès, 2011). In our case, the type A roots, the most expensive roots to
566 construct (because of their length and diameter), represented only 13.3% and 8.1% of
567 the lateral roots in pearl millet and maize, respectively. Thus, early growth cessation
568 could well be an important strategy to avoid an excessive cost of root system therefore
569 increasing the efficiency of each carbon molecule invested.
570
571 **The positioning of the three lateral root types is random along the primary root**
572 One benefit of the proposed approach is that it enables a model-based architectural
573 analysis. All lateral roots were assigned to types and precisely positioned along the
574 primary root. We showed that, both in pearl millet and maize, the longitudinal spacing
575 of lateral roots was highly variable, both within and between root systems. Our

analyses showed that there was no relationship between the length of the interval between two successive lateral roots and the types of these lateral roots and that the succession of lateral root types was random along the primary root. If confirmed, this would tend to rule out the hypothesis of a negative signal emanating from *e.g.* fast growing roots to prevent another fast growing root to grow in its neighborhood. Moreover, the absence of relationship between lateral root spacing and growth rate suggests that lateral root initiation and later development are regulated independently. These various hypotheses could be challenged using mutants affected in some of the hormonal (e.g., auxin or cytokinin)checkpoints associated with initiation (Lavenus et al., 2013).

A new experimental design is required for studying the whole growth profile of type A lateral roots

The experiment duration constrained by the rhizotron dimensions restricted observations to the beginning of type A lateral root growth. Hence, most of the growth rate profiles assigned to type A lateral roots were censored for both species. This makes a marked difference with type B and C lateral roots for which the whole growth profile, up to growth arrest, was observed for a large proportion of individuals. Hence, it would be useful to design larger rhizotrons or to change the growth conditions in order to study the whole growth of type A lateral roots and in particular the transition from increasing or stationary growth rate to decreasing growth rate. In order to capture such behavior, the proposed modeling framework can be directly extended by adding states in series for modeling successive growth phases for type A lateral roots. Such extension of semi-Markov switching models with states in series was recently developed for modeling successive developmental phase in Arabidopsis rosettes in Lièvre et al. (2016). We may expect a single state with decreasing growth rate following the current increasing growth rate state A or an intermediate roughly stationary growth state between the increasing and decreasing growth rate states. This would shed light on the future of “indeterminate” lateral roots which is to date not documented, contrary to the mechanisms associated with growth arrest (e.g. Varney and McCully, 1991). In particular, it would be interesting to see if this future interferes with the decay of primary root system reported in cereals, occurring for example within two months in pearl millet (Maiti and Bidinger, 1981).

An avenue for considering the diversity of lateral roots in future high-throughput phenotyping and genetic analyses

To date, genetic improvement based on structural features of the root system has essentially concentrated on its overall architecture such as deep vs. shallow rooting (Saengwilai et al., 2014) and on anatomy such as the presence of aerenchyma in maize roots, which are suspected to decrease the carbon construction cost of roots without affecting their function (Zhu et al., 2010). Lateral roots have been comparatively overlooked although they represent the best example of the overall structural plasticity of the root system to face the variable and unpredictable nature of the soil environment encountered (Drew, 1975). Therefore, there could exist a mine of genetic variation to exploit (and not only in cereals) if relevant phenotyping methods for characterizing the diversity of lateral roots were available. Depending on the environments for which genotypes are bred, it could be worth favoring or limiting the variability of lateral fates (Lynch 2018). By combining image analysis and statistical modeling, our phenotyping pipeline is a step in this direction.

Materials and Methods

Plant growth

Pearl millet (*Pennisetum glaucum* (L.) R. Br.) inbred lines LCICMB1 (Passot et al., 2016), maize (*Zea mays*) hybrid B73xUH007 (referred to as wild type) and *rtcs* mutants in the B73 background (Taramino et al., 2007; kindly provided by Frank Hochholdinger, University of Bonn, Germany) were used in this study. Root observation boxes (rhizotrons) were built according to Neufeld et al. (1989). The size of the frame was 40 cm x 70 cm so that they could be imaged with 2 contiguous A3 images using a scanner (Fig. 10). The root system was sandwiched against a plexiglass surface by a layer of viscose that was impermeable to roots, but permeable to water and nutrients. Rhizotrons were made of (back to front) a 5 mm thick extruded polystyrene plate, a 2 cm layer of substrate, a layer of viscose and a 5 mm thick plexiglass plate, all joined together using aluminum U frames held by screws. The substrate used was composed of 30% fine clay, 25% peat fibers, 5% blond peat and

40% frozen black peat (Klasmann-Deilmann France SARL). The substrate was sieved before using. The rhizotrons were weighed individually before and after filling to determine the weight of substrate contained in each one and later to manage daily irrigation.

Maize seeds were surface sterilized with 6% hypochlorite for five minutes and rinsed in distilled water for one minute. Seeds were then germinated on moistened filter paper in Petri-dishes (20 x 20 cm) and placed vertically in a growth chamber in the dark at 20°C. Pearl millet germination was performed with a similar protocol, except that seeds were also cleaned with ethanol solution (70%) for 5 minutes after the first rinsing and germination temperature was set to 30°C. Germinated seedlings with similar primary root length were transferred individually in the rhizotrons. A layer of wet sphagnum on the top of the rhizotrons maintained the seedlings and prevented them from drying. Rhizotrons were placed in a growth room with climatic conditions adapted to each species: a temperature of 28°C during the day and 24°C during the night for pearl millet and a constant temperature of 20°C for maize, with a 14-hour-photoperiod for both species. Light was provided by 6 mercury lamps (HQI, 250 W, Osram, Munich, Germany) and measured by a light sensor (SKP215, Skye Instruments, Llandrindod Wells, Powys, UK). In our conditions, photosynthetic photon flux density (PPFD) was 300 µmol/m²/s. Temperature and air humidity were recorded (HC2-SH, Rotronic, Bassersdorf, CH) for each growth room. The sphagnum was watered twice a day at the beginning of the experiment and from 6 days after germination onward, rhizotrons were watered daily using a 1/10 Hoagland solution to maintain the humidity of the substrate. The amount of watering was monitored by a daily weighting of the rhizotron. In one experiment, plants were shaded by installing a net above the plants that reduced light intensity by 75%.

Imaging and image processing

From the second day of growth, rhizotrons were scanned with an A3 scanner (Epson Expression 10000XL Pro, Japan) at 600 or 720 dpi. The histogram of the gray level intensities was adjusted to optimize the contrast on fine roots. As rhizotrons are twice the size of the scanner, two images (upper part and lower part of the rhizotron) were taken and aligned using Align_4 (http://www.mecourse.com/landinig/software/

software.html) to recover an image of the entire root system, thanks to landmarks visible in both parts. These landmarks were either added intentionally on the rhizotron or were naturally present (water drops, the root system itself).

The SmartRoot software (Lobet et al., 2011) was used to extract root system architecture at successive dates as well as root growth parameters because it supports time-lapse images and focuses on the analysis of individual root behavior. SmartRoot needs images where roots appear darker than background. An ImageJ (Rasband, W.S., U. S. National Institutes of Health, Bethesda, Maryland, USA) macro was developed to automatically invert and adjust the contrast of the rhizotron images by scaling the image intensity histogram on a fixed range. The optimal contrast (min and max values of the intensity range) was determined empirically to reduce the number of errors when using the algorithm for automatic lateral root tracing provided by SmartRoot using a subset of scan images, and was applied to the whole set of images using the macro tool.

SmartRoot enables semi-automatic root tracing. The primary root was drawn on the first image. For the next days, the root system traced on the previous day was imported and aligned, in such a way that the trace of the primary root elongated progressively, using automatic tracing. Crown and lateral roots were added as they appeared, either manually or using automatic detection. Their lengths increased progressively on the successive scans as for the primary root. When all roots were traced, the data were extracted with the batch export tool of SmartRoot. This tool provides several measurements including the length, the insertion position and the diameter for each root. The growth rates were directly extracted from successive length measurement. Because the resolution was not sufficient for pearl millet lateral roots, we only considered root diameter for maize. On average, it took about two days to process the data of one plant.

Correction of growth rate profiles

In spite of manual supervision of root tracings, the exported dataset contained some digitalization errors. It was therefore necessary to characterize the implausible data points resulting from such errors and to clean out the dataset. We designed a data

correction algorithm aiming at identifying implausible growth rate profiles that derive from errors in image analysis. The most typical errors were defaults in alignment, one-day missing root length increments or non-visible root tips in the case of roots encountering an obstacle. This kind of error results in implausible trajectories for the root length at some time point, which can be better identified by examining growth rate profiles. Depending on the type of error, growth rate profiles were either corrected or truncated before the first implausible growth rate. The data correction algorithm is described in Supplemental Methods S3.

Statistical models

Definition of semi-Markov switching linear models

Semi-Markov switching linear models are two-scale models that generalize hidden semi-Markov chains by incorporating linear regression models as observation models. They are formally defined in Supplemental Methods S1. In our context, the succession and duration of growth phases (coarse scale) are represented by a non-observable semi-Markov chain while the growth rate trend within a growth phase (fine scale) are represented by observation linear models attached to each state of the semi-Markov chain. Hence, each state of the semi-Markov chain represents a growth phase. A *J*-state semi-Markov chain is defined by three subsets of parameters:

1. Initial probabilities $(\pi_j; j = 0, \ldots, J-1)$ to model which is the first phase occurring in a growth rate profile,
2. Transition probabilities $(p_{ij}; i, j = 0, \ldots, J-1)$ to model the succession of growth phases,
3. Occupancy distributions attached to non-absorbing states (a state is said to be absorbing if, after entering this state, it is impossible to leave it) to model the growth phase duration in number of days. We used, as possible parametric state occupancy distributions binomial distributions B(d, n, p), Poisson distributions P(d, λ) and negative binomial distributions NB(d, r, p) with an additional shift parameter $d \geq 1$.

A SMS-LM adds observation linear models to the non-observable semi-Markov chain:

4. We chose to model growth rate trends within growth phases using simple linear regression models because of the short length of growth phases (up to 10

successive growth rates for pearl millet and up to 17 successive growth rates for maize).

A SMS-LM composed of parallel transient states followed by a final absorbing state was estimated on the basis of growth rate profiles corresponding to a given species. A state is said to be transient if after leaving this state, it is impossible to return to it. The parallel transient states represent alternative growth phases. The final absorbing state represents the growth arrest and a degenerate linear model corresponding to a constant null growth rate is associated with this state. The censoring level was computed for each growth state as a by-product of the estimation of the corresponding growth phase duration distribution within SMS-LM. This censoring level takes into account all the possible assignments of growth rate profiles of length ≥ 5 incorporated in the learning sample. Each estimated model was used to compute the most probable state series for each observed growth rate profile (Guédon, 2003). This restored state series can be viewed as the optimal segmentation of the corresponding observed series into at most two sub-series corresponding to a given growth phase either censored or followed by a growth arrest. Because of the transient growth states in parallel, this restoration can be interpreted as a classification of the lateral roots on the basis of their growth rate profiles. In the case of the maize *rtcs* mutant and the shading treatment, the growth rate profiles were segmented using both the model estimated on the corresponding growth rate profiles and the unshaded wild-type model.

Definition of stationary variable-order Markov chain

Most of the methods for analyzing local dependencies in discrete sequences rely on high-order Markov chains. However, the number of free parameters of a Markov chain increases exponentially with its order, i.e. with the memory length taken into account. For instance, in the case of three states (corresponding to three lateral root types), the number of free parameters is 2 for a zero-order, 6 for a first-order, 18 for a second-order Markov chain, etc. Since there are no models "in between", this very discontinuous increase in the number of free parameters causes the estimated high-order Markov chains to be generally over-parameterized. This drawback can be overcome by defining sub-classes of parsimonious high-order Markov chains such as variable-order Markov chains (Ron et al., 1997; Bühlmann and Wyner, 1999) where the order is variable and depends on the "context" within the sequences, instead of

being fixed. Stationary variable-order Markov chains are formally defined in Supplemental Methods S4.

Pearl millet root anatomy

Plants were grown in rhizotrons as previously described. Lateral root growth rate profiles were extracted before sampling, to determine the type of each root. Sampling was performed around 15 days after germination. Selected roots were harvested and fixed overnight in an acetic acid: ethanol solution (1:9) and conserved in 70% ethanol. Segments were taken around the middle of each lateral root. Root segments were gently dried on a filter paper and imbibed in warm (30-45°C) liquid 3% agarose solution (SeaKem GTG Agarose, Lonza). Then, 55 µm-thick sections were obtained from solidified agarose blocks using a vibratome (Microm HM 650V, Thermo Scientific, speed 30, frequency 60). Individual root sections were then collected, transferred to microscope slides and covered with a coverslip for direct observation.

Images were taken using a Leica DMRB microscope equipped with an epifluorescence filter (excitation range: UV; excitation filter: 460-480 nm). Two pictures were taken for each root section: one under visible light using Nomarsky optics and another using epifluorescence that takes advantage of the natural fluorescence of cell walls with secondary deposits. Images were taken using a Retiga SRV FAST 1394 camera and the QCapture Pro7 software. The RGB images were opened in ImageJ using the Bioformats importer plugin and transformed in gray level 8-bit images. A scale-bar was added to the images according to their magnification. Measurements of the diameter, stele and metaxylem and the number of xylem poles and vessels were recorded for each root section.

Supplemental Data

Supplemental Figure S1. Four-state semi-Markov switching linear model estimated on the basis of maize lateral root growth rate profiles.

Supplemental Figure S2. Daily median growth rates of lateral roots in pearl millet.

Supplemental Figure S3. Ranked posterior probabilities of the optimal assignment of each lateral root growth rate profile of length ≥ 5 to a cluster.

Supplemental Figure S4. Cumulative distribution functions of the length of lateral root growth rate profiles.

Supplemental Figure S5. Ranked posterior probabilities of the optimal assignment of each lateral root growth rate profile of length < 5 to a cluster.

Supplemental Figure S6. Daily median growth rates and apical diameters of lateral roots in maize *rtcs* mutants.

Supplemental Figure S7. Daily median growth rates and apical diameters of lateral roots in shaded maize.

Supplemental Figure S8. Spearman rank autocorrelation functions in pearl millet and maize.

Supplemental Figure S9. Distributions of the length of intervals between successive lateral roots.

Supplemental Table S1. Overlaps between growth rate distributions corresponding to lateral root clusters for pearl millet.

Supplemental Table S2. Overlaps between growth rate distributions corresponding to lateral root clusters for maize.

Supplemental Table S3. Overlaps between growth rate distributions and apical diameter distributions corresponding to lateral root types for maize.

Supplemental Table S4. Length of the intervals between successive lateral roots in pearl millet.

Supplemental Table S5. Length of the intervals between successive lateral roots in maize.

Supplemental Methods S1. Definition of semi-Markov switching linear models and associated statistical methods.

Supplemental Methods S2. Empirical selection of the number of clusters of lateral roots.

Supplemental Methods S3. Algorithm for correcting growth rate profiles.

Supplemental Methods S4. Definition of stationary variable-order Markov chains and associated statistical methods.

Table 1. Characteristics (mean and standard deviation (s.d.) in days; and censoring level (c.l.; %)) of growth phase duration distributions estimated for the three root types within the semi-Markov switching linear models for pearl millet and maize (wild-type plants, *rtcs* mutant and wild-type plants exposed to shading).

	Pearl millet			Maize								
				Wild type			*rtcs* mutant			Shading		
Root type	mean	s.d.	c.l.	mean	s.d.	c.l.	mean	s.d.	c.l.	mean	s.d.	c.l.
A	17.3	7.6	96.2	15.2	7.7	80.3	15.7	8.6	89.7			
B	7.6	4.6	53.6	6.9	5	36.3	5.8	3.3	37	5.8	3	25.6
C	3.2	2.6	13.9	3	2.4	9.7	2.9	1.9	5.1	2.5	1.7	2.5

Table 2. Proportions (%) of lateral root types in the pearl millet and maize (wild-type plants, *rtcs* mutant and wild-type plants exposed to shading).

	Pearl millet	Maize		
Root type		Wild type	*rtcs* mutant	Shading
A	13.3	8.1	8	
B	23.8	27.3	34.4	26
C	62.9	64.6	57.6	74

Table 3. Length of the intervals between successive lateral roots classified according to the type of the lateral roots delimiting the interval in the shootward direction (sample size, mean and standard deviation (s.d.) in mm for each type). No significant differences between the means were found (ANOVA, $p = 0.83$ and $p = 0.33$ for pearl millet and maize, respectively).

	Pearl millet			Maize		
Root type	A	B	C	A	B	C
Sample size	165	296	785	249	830	1958
Mean	2.2	2.1	2.1	1.6	1.6	1.7
s.d.	2.7	2.7	1.9	1.6	1.5	1.5

List of Figures

Figure 1. Growth rate profiles of lateral roots. Lateral roots of (A) one pearl millet and (B) one maize plant were assigned to the lateral root types, A, B and C using the estimated semi-Markov switching linear models. Root age refers to the number of days following emergence.

Figure 2. Four-state semi-Markov switching linear model estimated on the basis of pearl millet lateral root growth rate profiles. The three growth states correspond to the lateral root types, A, B and C, and the "end" state to growth arrest. (A) Growth phase duration distributions; (B) Graph of transitions. The possible transitions between states are represented by arcs (the attached probabilities are always equal to 1). The arcs entering in states indicate initial states and the attached initial probabilities are noted nearby. (C) Linear trend models estimated for each state.

Figure 3. Growth phase duration distributions in pearl millet and maize. Distributions were estimated for lateral root types A, B and C within the 4-state semi-Markov switching linear model for (A) pearl millet and (B) maize. The relative frequency distributions of the length of growth rate profiles are drawn for illustrating the censoring level. Only lengths ≥ 5 corresponding to lateral roots used to build the semi-Markov switching linear models are shown.

Figure 4. Ranked posterior probabilities of the optimal assignment of each lateral root growth rate profile to a cluster. Growth rate profiles were truncated at length 1, 2, 3 and 5, or left untruncated for (A) pearl millet and (B) maize.

Figure 5. Daily median growth rates and apical diameters of lateral roots in pearl millet and maize. Daily median growth rates and associated mean absolute deviations (m.a.d.) were computed for (A) pearl millet and (B) maize lateral root types A, B and C. (C) Daily median apical diameters and associated m.a.d. were computed for maize lateral root types A, B and C.

Figure 6. Relationship between stele and central xylem tracheary element (XTE) diameter of lateral roots in pearl millet. Colors indicate the lateral root types determined on the basis of the assignment of growth rate profiles using semi-Markov switching linear models.

Figure 7. Growth phase duration distributions in wild-type, *rtcs* mutant and shaded maize. Distributions were estimated for lateral root types A, B and C within the semi-Markov switching linear model for the (A) wild-type, (B) *rtcs* mutant and (C) shaded maize. The relative frequency distributions of the length of growth rate profiles are drawn for illustrating the censoring level. Only lengths ≥ 5 corresponding to lateral roots used to build the semi-Markov switching linear models are shown.

Figure 8. Daily median growth rates and apical diameters of lateral roots in wild-type, *rtcs* mutant and shaded maize. (A) Daily median growth rates and (B) apical diameters were computed for lateral root types A, B and C of wild-type, *rtcs* mutant and shaded maize.

Figure 9. Proportions of lateral root types. Proportions are shown for each (A) pearl millet and (B) maize plant. Plants were assigned to groups (indicated by letters) using the Kruskal-Wallis test. Bin areas are proportional to the number of lateral roots of each type. Bin widths are proportional to the total number of lateral roots per plant (indicated below each bin).

Figure 10. Rhizotron development and root system measurement. Root observation boxes (rhizotrons) were built according to Neufeld et al. (1989). (A, B) Rhizotrons were made of (back to front) an extruded polystyrene plate, a layer of substrate (sieved peat and compost), a layer of viscose (impermeable to roots, but permeable to water and nutrients) and plexiglass plate, all joined together using aluminum U frames held by screws. Germinated seedlings with similar primary root length were transferred individually. A layer of wet sphagnum on the top of the rhizotrons maintained the seedlings and prevented them from drying. Rhizotrons were placed in a growth room with climatic conditions adapted to each species. Rhizotrons were daily scanned with an A3 scanner. (C) The SmartRoot software (Lobet et al., 2011) was used to extract root system architecture at successive dates and compute root growth parameters.

Acknowledgments

The authors thank Gaëlle Rolland for her help during plant phenotyping using SmartRoot, Xavier Draye for fruitful discussions and Frank Hochholdinger for providing the *rtcs* seeds.

Literature cited

Aguirrezabal LAN, Deleens E, Tardieu F (1994). Root elongation rate is accounted for by intercepted PPFD and source-sink relations in field and laboratory-grown sunflower. Plant, Cell Environ. 17: 443–450.

Aschehoug ET, Callaway RM (2014). Morphological variability in tree root architecture indirectly affects coexistence among competitors in the understory. Ecology 95: 1731–1736.

Atkinson JA, Wingen LU, Griffiths M, Pound MP, Gaju O, Foulkes MJ, Le Gouis J, Griffiths S, Bennett MJ, King J. (2015). Phenotyping pipeline reveals major seedling root growth QTL in hexaploid wheat. J. Exp. Bot. 66: 2283–2292.

Bingham IJ, Stevenson EA (1993). Control of root growth: effects of carbohydrates on the extension, branching and rate of respiration of different fractions of wheat roots. Physiol. Plantarum 88: 149–158.

Bishopp A, Lynch JP (2015). The hidden half of crop yields. Nat. Plants 1: 15117.

Bühlmann P, Wyner AJ (1999). Variable length Markov chains. Ann. Stat. 27: 480–513.

Coutts MP (1987). Developmental processes in tree root systems. Can. J. For. Res. 17: 761–767.

Csiszár I, Talata Z (2006). Context tree estimation for not necessarily finite memory processes, Via BIC and MDL. IEEE Trans. Inf. Theory 52: 1007–1016.

De Smet I, Signora L, Beeckman T, Inzé D, Foyer CH, Zhang H (2003). An abscisic acid-sensitive checkpoint in lateral root development of Arabidopsis. Plant J. 33: 543–555.

Dhondt S, Wuyts N, Inzé D (2013). Cell to whole-plant phenotyping: The best is yet to come. Trends Plant Sci. 18: 1360–1385.

Drew MC (1975). Comparison of the effects of a localized supply of phosphate, nitrate, ammonium and potassium on the growth of the seminal root sytem, and the shoot, in barley. New Phytol. 75: 479–490.

Fahlgren N, Feldman M, Gehan MA, Wilson MS, Shyu C, Bryant DW, Hill ST, McEntee CJ, Warnasooriya SN, Kumar I, et al (2015a). A versatile phenotyping system and analytics platform reveals diverse temporal responses to water availability in *Setaria*. Mol. Plant 8: 1520–1535.

Fahlgren N, Gehan MA, Baxter I (2015b). Lights, camera, action: high-throughput plant phenotyping is ready for a close-up. Curr. Opin. Plant Biol. 24: 93–99.

Farrar JF, Jones CL (1986). Modification of respiration and carbohydrate status of barley roots by selective pruning. New Phytol. 102: 513–521.

Forde BG (2009). Is it good noise? The role of developmental instability in the shaping of a root system. J. Exp. Bot. 60, 3989–4002.

Freixes S, Thibaud M-C, Tardieu F, Muller B (2002). Root elongation and branching is related to local hexose concentration in *Arabidopsis thaliana* seedlings. Plant, Cell Environ. 25: 1357–1366.

Gowda VRP, Henry A, Yamauchi A, Shashidhar HE, Serraj R (2011). Root biology and genetic improvement for drought avoidance in rice. Field Crops Res. 122: 1–13.

Guédon Y (2003). Estimating hidden semi-Markov chains fom discrete sequences. J. Comput. Graph. Stat. 12: 604–639.

Henry S, Divol F, Bettembourg M, Bureau C, Guiderdoni E, Périn C, Dievart A (2016). Immunoprofiling of rice root cortex reveals two cortical subdomains. Front. Plant Sci. 6: 1–9.

Hetz W, Hochholdinger F, Schwall M, Feix G (1996). Isolation and characterization of rtcs, a maize mutant deficient in the formation of nodal roots. Plant J. 10: 845–857.

Iyer-Pascuzzi, AS, Symonova O, Mileyko Y, Hao Y, Belcher H, Harer J, Weitz JS, Benfey PN (2010). Imaging and analysis platform for automatic phenotyping and trait ranking of plant root systems. Plant Physiol. 152: 1148–1157.

Jordan MO, Harada J, Bruchou C, Yamazaki K (1993). Maize nodal root ramification: Absence of dormant primordia, root classification using histological parameters and consequences on sap conduction. Plant Soil 153: 125–143.

Kuijken RCP, van Eeuwijk FA, Marcelis LFM, Bouwmeester HJ (2015). Root phenotyping: from component trait in the lab to breeding. J. Exp. Bot. 66: 5389–5401.

Lavenus J, Goh T, Roberts I, Guyomarc'h S, Lucas M, De Smet I, Fukaki H, Beeckman T, Bennett M, Laplaze L (2013). Lateral root development in *Arabidopsis*: fifty shades of auxin. Trends Plant Sci., 18: 450–458.

Lecompte F, Pagès L, Ozier-Lafontaine H (2005). Patterns of variability in the diameter of lateral roots in the banana root system. New Phytol. 167: 841–850.

Lièvre M, Granier C, Guédon Y (2016). Identifying developmental phases in the *Arabidopsis thaliana* rosette using integrative segmentation models. New Phytol. 210: 1466–1478.

Lobet G, Pagès L, Draye X (2011). A novel image-analysis toolbox enabling quantitative analysis of root system architecture. Plant Physiol. 157: 29–39.

Lynch JP. (2018) Rightsizing root phenotypes for drought resistance. J. Exp. Bot. in press.

MacLeod RD (1990). Lateral root primordium inception in Zea mays L. Environ. Exp. Bot. 30: 225–234.

Maiti RK, Bidinger FR (1981). Growth and development of the pearl millet plant. ICRISAT Res. Bull. 6.

Malamy JE (2005). Intrinsic and environmental response pathways that regulate root system architecture. Plant, Cell Environ. 28: 67–77.

Moreno-Ortega B, Fort G, Muller B, Guédon Y (2017). Identifying developmental zones in maize lateral root cell length profiles using multiple change-point models. Front. Plant Sci. 8: 1750.

Muller B, Stosser M, Tardieu F (1998). Spatial distributions of tissue expansion and cell division rates are related to irradiance and to sugar content in the growing zone of maize roots. Plant, Cell Environ. 21: 149–158.

Nestler J, Keyes SD, Wissuwa M. (2016). Root hair formation in rice (*Oryza sativa* L.) differs between root types and is altered in artificial growth conditions. J Exp. Bot. 67: 3699–3708.

Neufeld HS, Durall DM, Rich PM, Tingey DT (1989). A rootbox for quantitative observations on intact entire root systems. Plant Soil 117: 295–298.

Pagès L (1995). Growth patterns of the lateral roots of young oak (*Quercus robur*) tree seedlings Relationship with apical diameter. New Phytol. 130: 503–509.

Pagès L (2011). Links between root developmental traits and foraging performance. Plant. Cell Environ. 34 : 1749–1760.

Passot S, Gnacko F, Moukouanga D, Lucas M, Guyomarc'h S, Moreno Ortega B, Atkinson JA, Belko MN, Bennett MJ, Gantet P et al (2016). Characterization of pearl millet root architecture and anatomy reveals three types of lateral roots. Front. Plant Sci. 7: 1–11.

Rebouillat J, Dievart A, Verdeil JL, Escoute J, Giese G, Breitler JC, Gantet P, Espeout S, Guiderdoni E, Périn C (2009). Molecular genetics of rice root development. Rice 2: 15–34.

Ron D, Singer Y, Tishby N (1997). The power of amnesia: Learning probabilistic automata with variable memory length. Mach. Learn. 25: 117–149.

Saengwilai P, Tian X, Lynch JP (2014). Low crown root number enhances nitrogen acquisition from low-nitrogen soils in maize. Plant Physiol. 166: 581–589.

Taramino G, Sauer M, Stauffer JL, Multani D, Niu X., Sakai H, Hochholdinger F (2007). The maize (*Zea mays* L.) RTCS gene encodes a LOB domain protein that is a key regulator of embryonic seminal and post-embryonic shoot-borne root initiation. Plant J. 50: 649-659.

Thaler P, Pagès L (1996). Root apical diameter and root elongation rate of rubber seedlings (*Hevea brasiliensis*) show parallel responses to photoassimilate availability. Physiol. Plant. 97: 365–371.

Topp CN, Iyer-Pascuzzi AS, Anderson JT, Lee C-R, Zurek PR, Symonova O, Zheng Y, Bucksch A, Mileyko Y, Galkovskyi T, et al (2013). 3D phenotyping and quantitative trait

locus mapping identify core regions of the rice genome controlling root architecture. Proc. Natl. Acad. Sci. U. S. A. 110: E1695–704.

Varney GT, Canny MJ, Wang XL, McCully ME (1991). The branch roots of Zea. I. First order branches, their number, sizes and division into classes. Ann. Bot. 67: 357–364.

Varney GT, McCully, ME (1991). The branch roots of Zea. II. Developmental loss of the apical meristem in field-grown roots. New Phytol. 118: 535–546.

Vejchasarn P, Lynch JP, Brown KM. (2016). Genetic variability in phosphorus responses of rice root phenotypes. Rice 9: 29.

Wang XL, McCully ME, Canny MJ. (1994). The branch roots of *Zea*. IV. The maturation and openness of xylem conduits in first-order branches of soil-grown roots. New Phytol. 126: 21–29.

Watt M, Magee LJ, McCully, ME (2008). Types, structure and potential for axial water flow in the deepest roots of field-grown cereals. New Phytol. 178: 135–146.

Williamson LC, Ribrioux SPCP, Fitter AH, Leyser HMO (2001). Phosphate Availability Regulates Root System Architecture in Arabidopsis. Plant Physiol. 126: 875–882.

Wu Q, Pagès L, Wu J (2016). Relationships between root diameter, root length and root branching along lateral roots in adult, field-grown maize. Ann. Bot. 117:379–390.

Zhu J, Brown KM, Lynch JP (2010). Root cortical aerenchyma improves the drought tolerance of maize (*Zea mays* L.). Plant, Cell Environ. 33: 740–749.

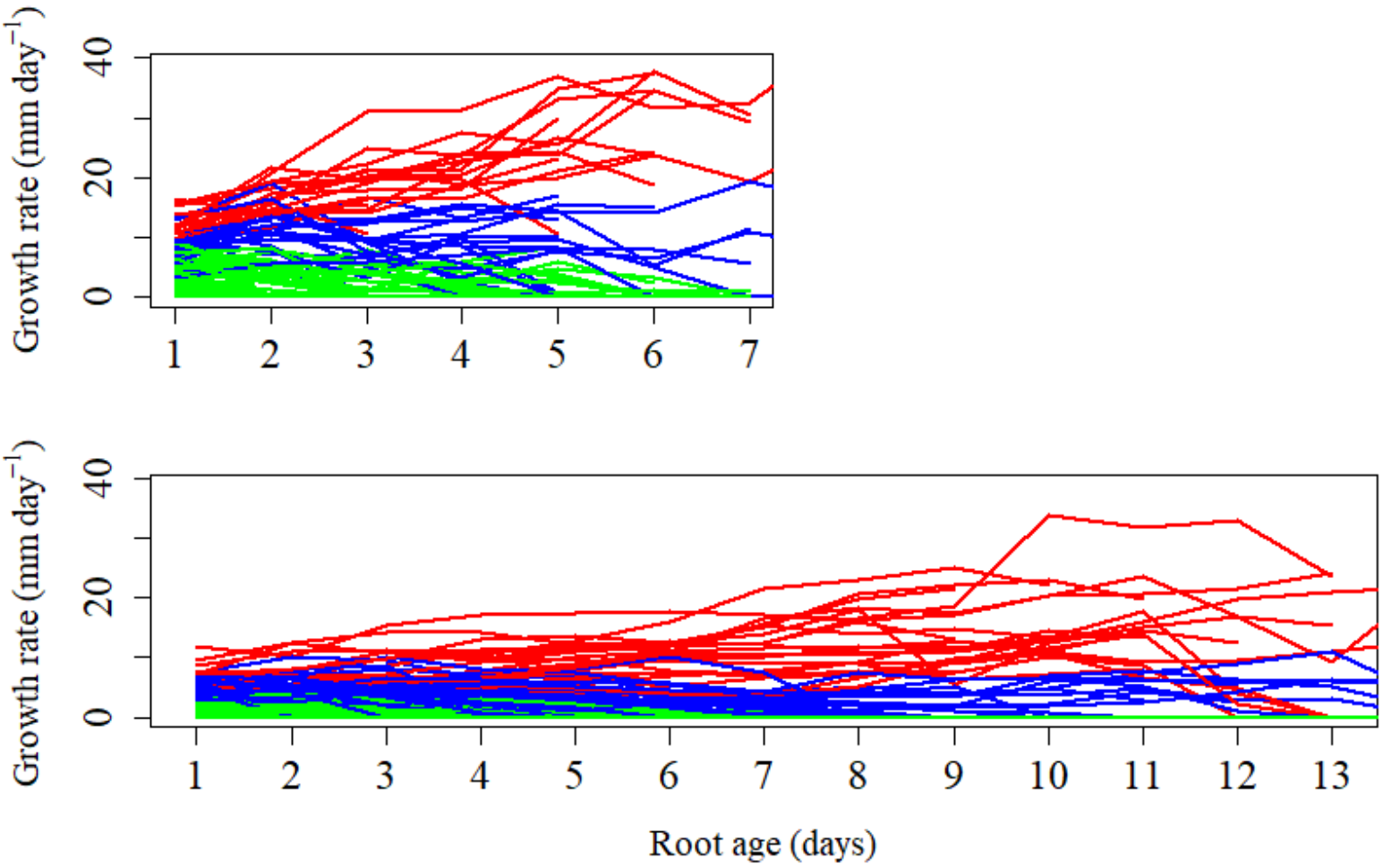

Figure 1. Growth rate profiles of lateral roots

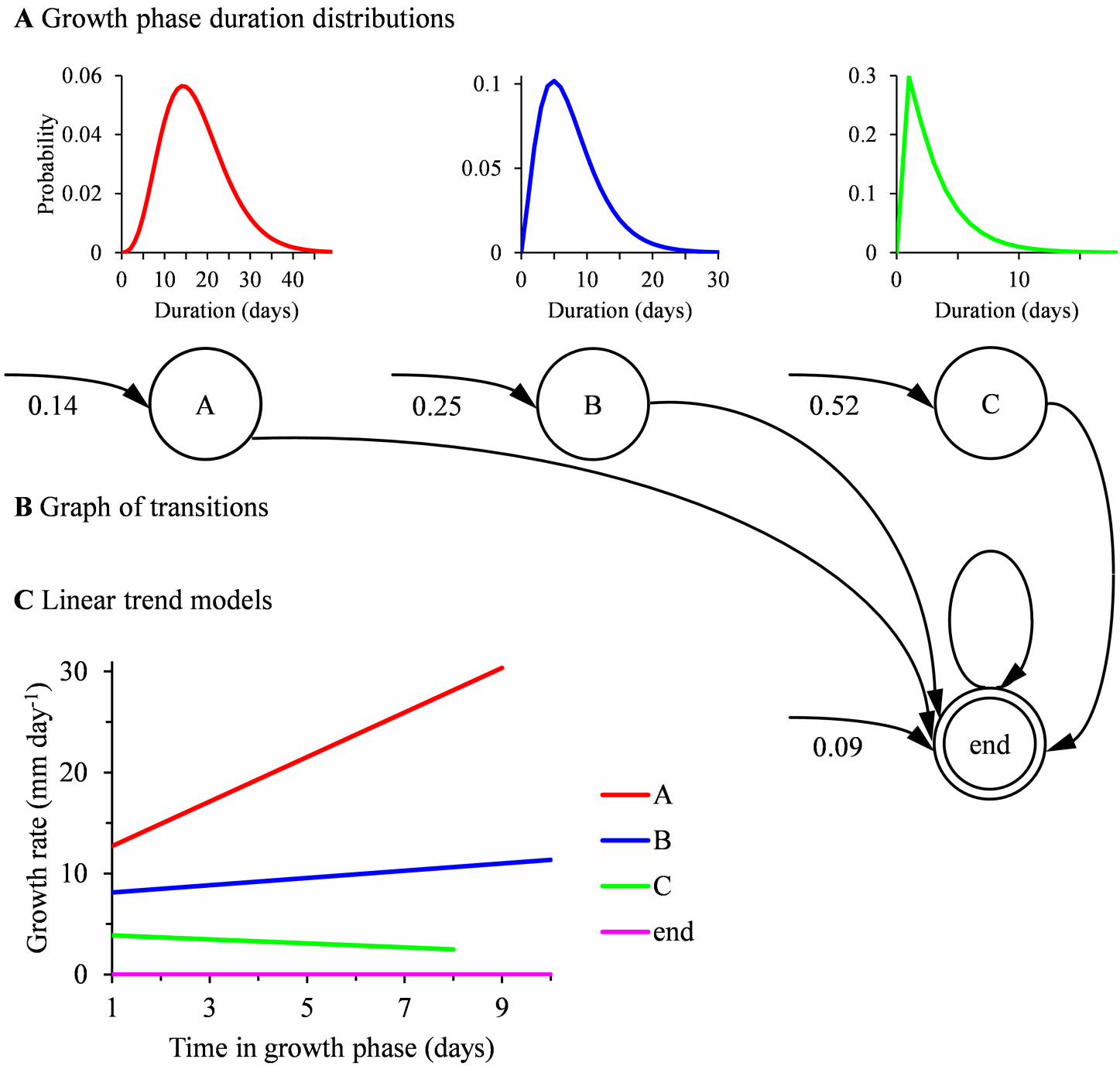

Figure 2. Four-state semi-Markov switching linear model estimated on the basis of pearl millet lateral root growth rate profiles.

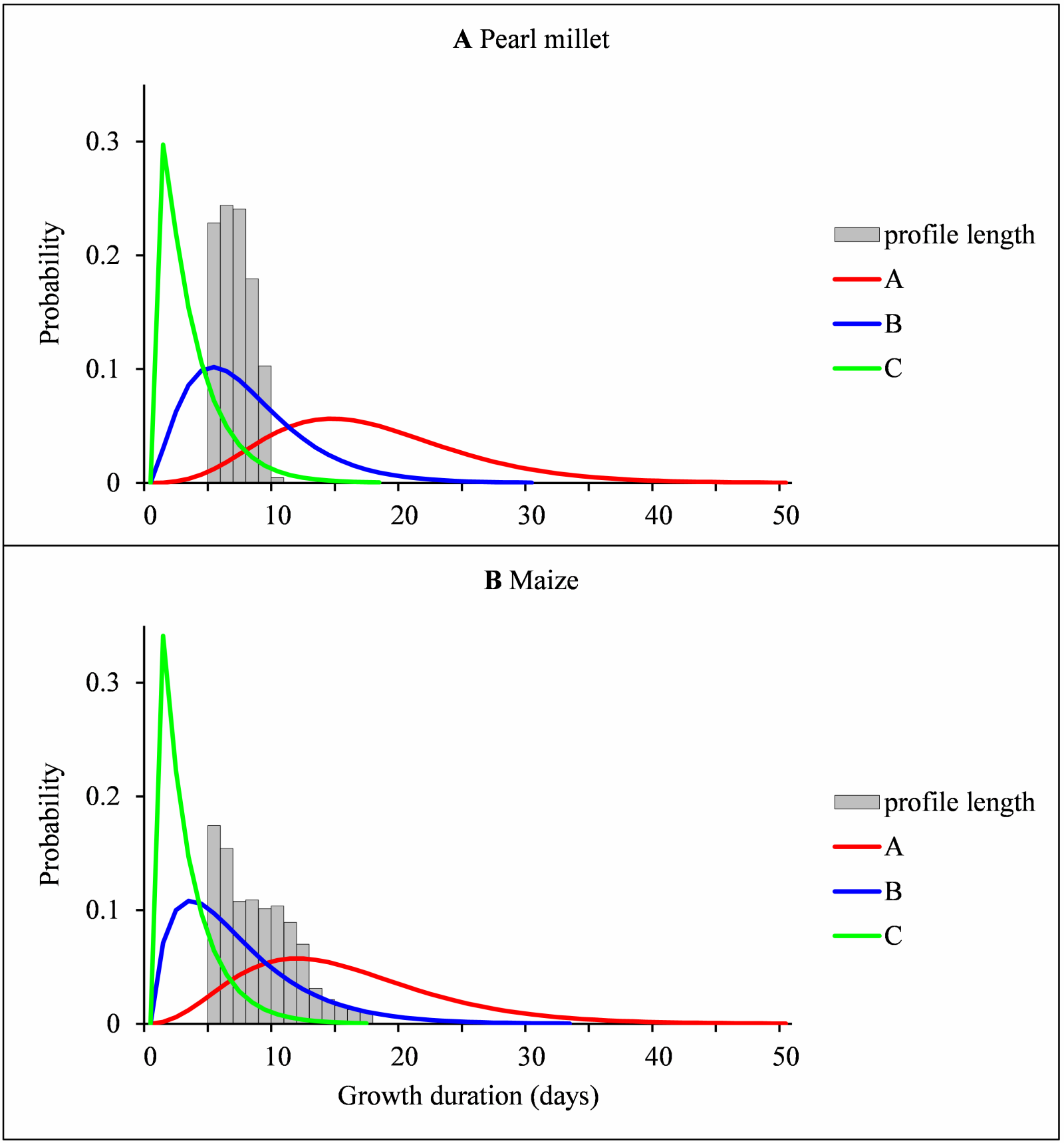

Figure 3. Growth phase duration distributions in pearl millet and maize.

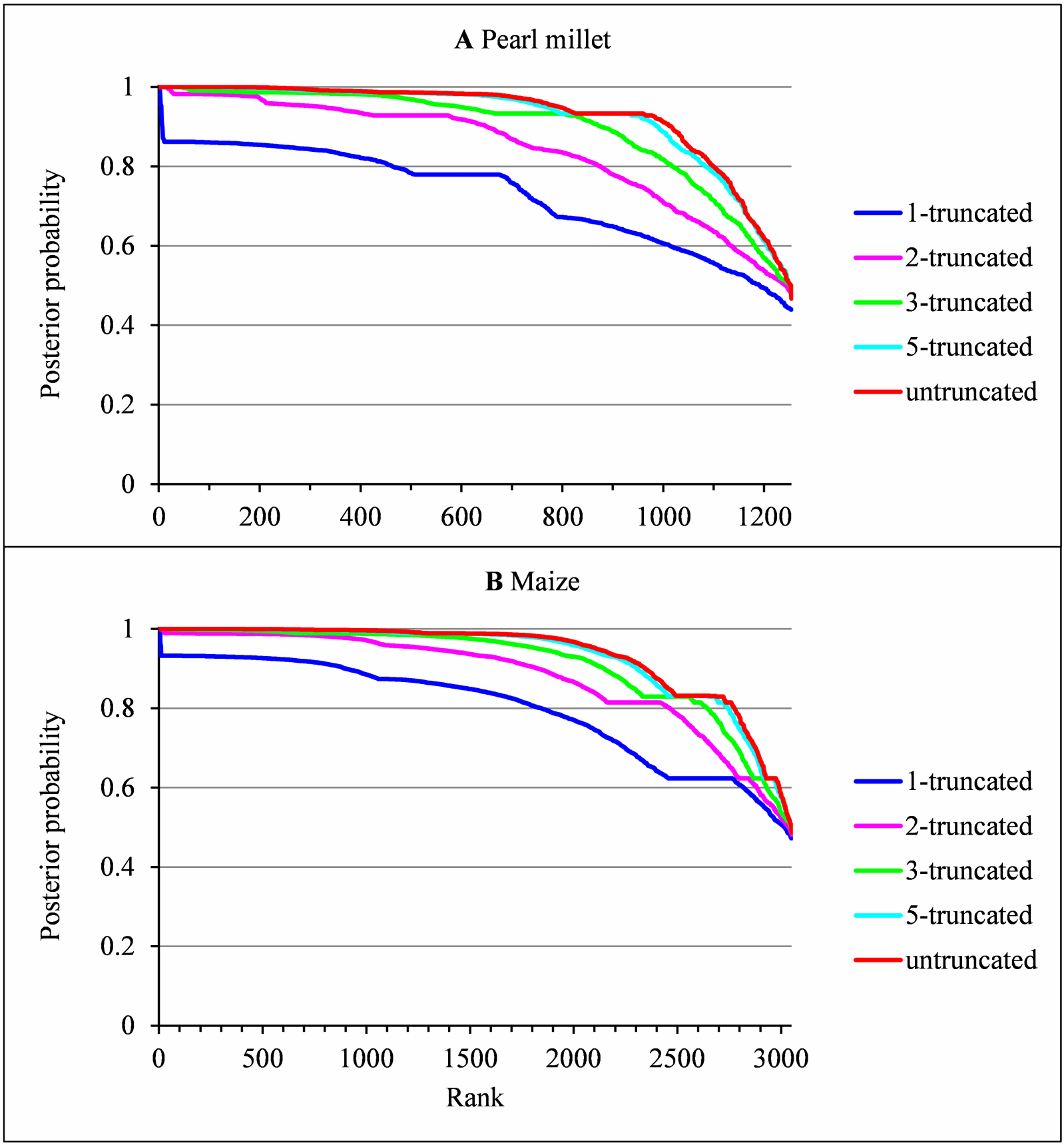

Figure 4. Ranked posterior probabilities of the optimal assignment of each lateral root growth rate profile to a cluster.

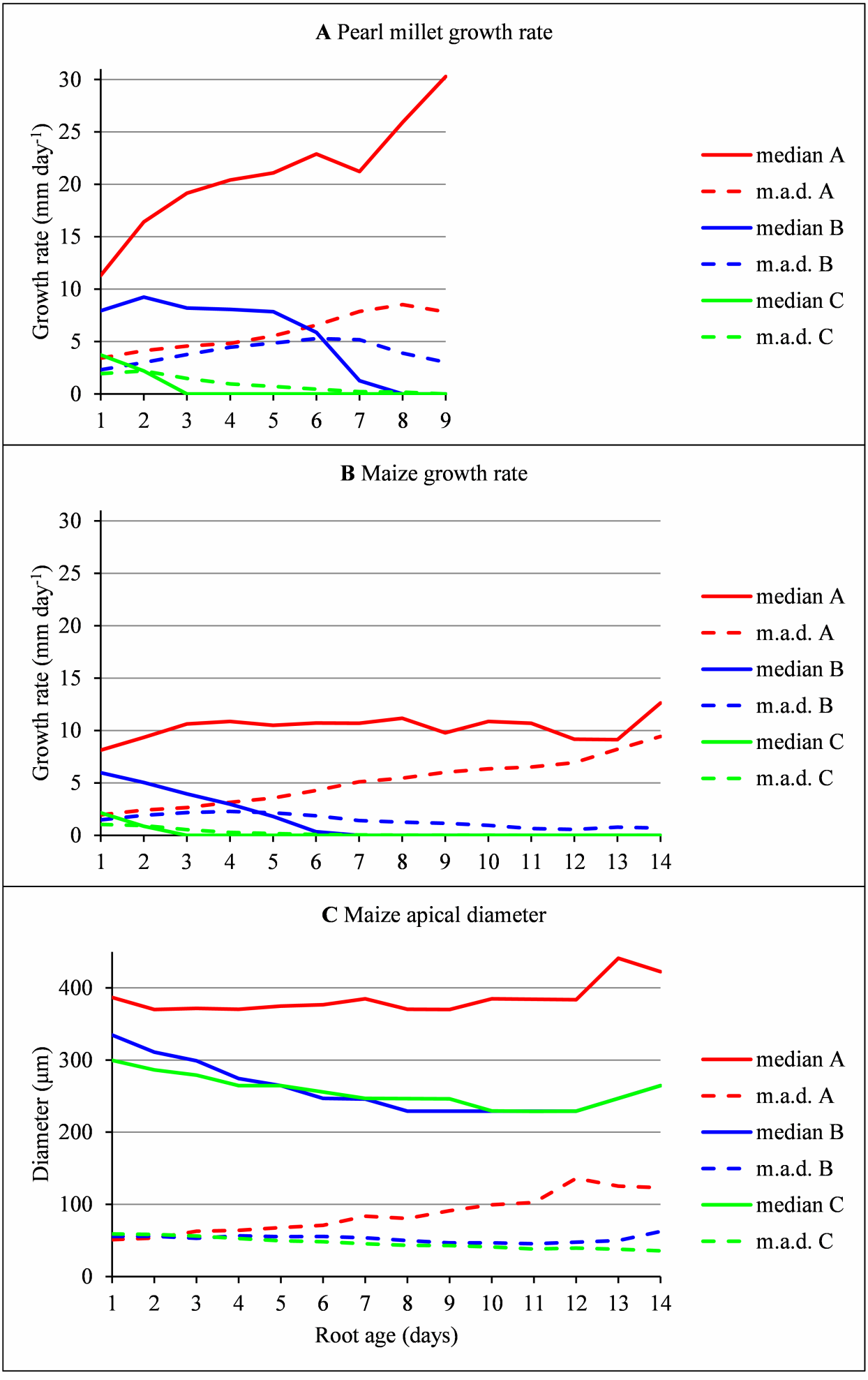

Figure 5. Daily median growth rates and apical diameters of lateral roots in pearl millet and maize.

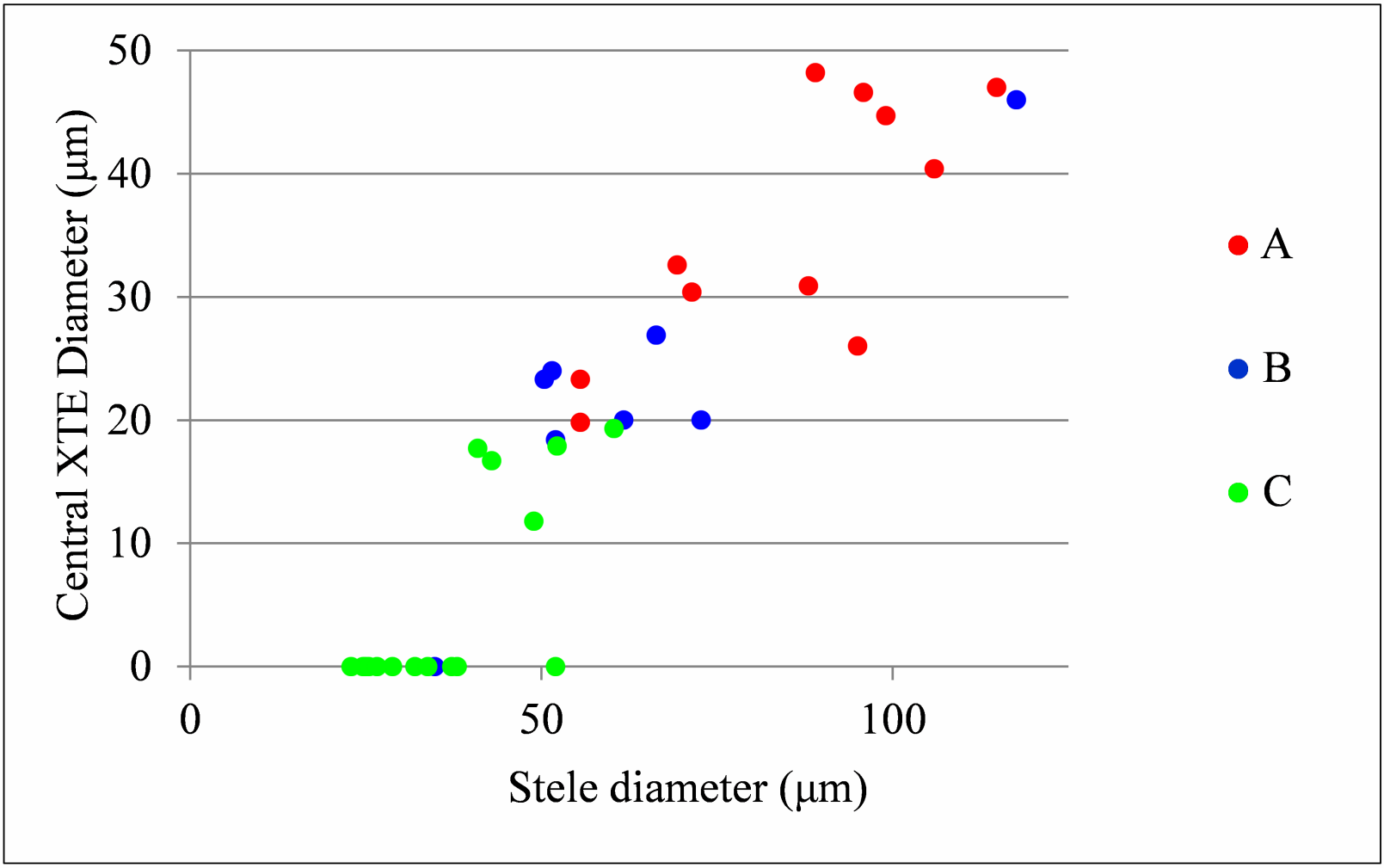

Figure 6. Relationship between stele and central xylem tracheary element (XTE) diameter of lateral roots in pearl millet.

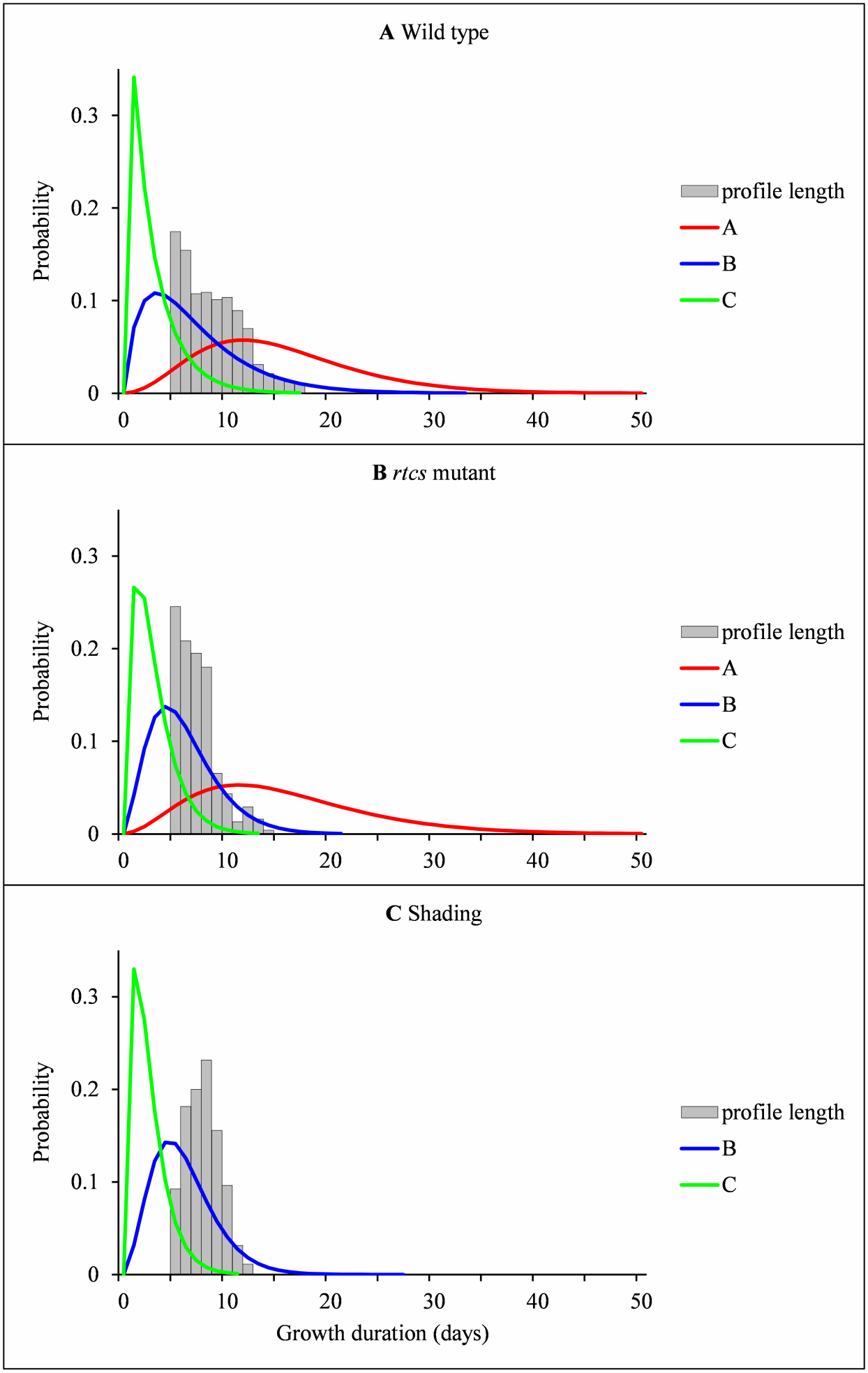

Figure 7. Growth phase duration distributions in wild-type, *rtcs* mutant and shaded maize.

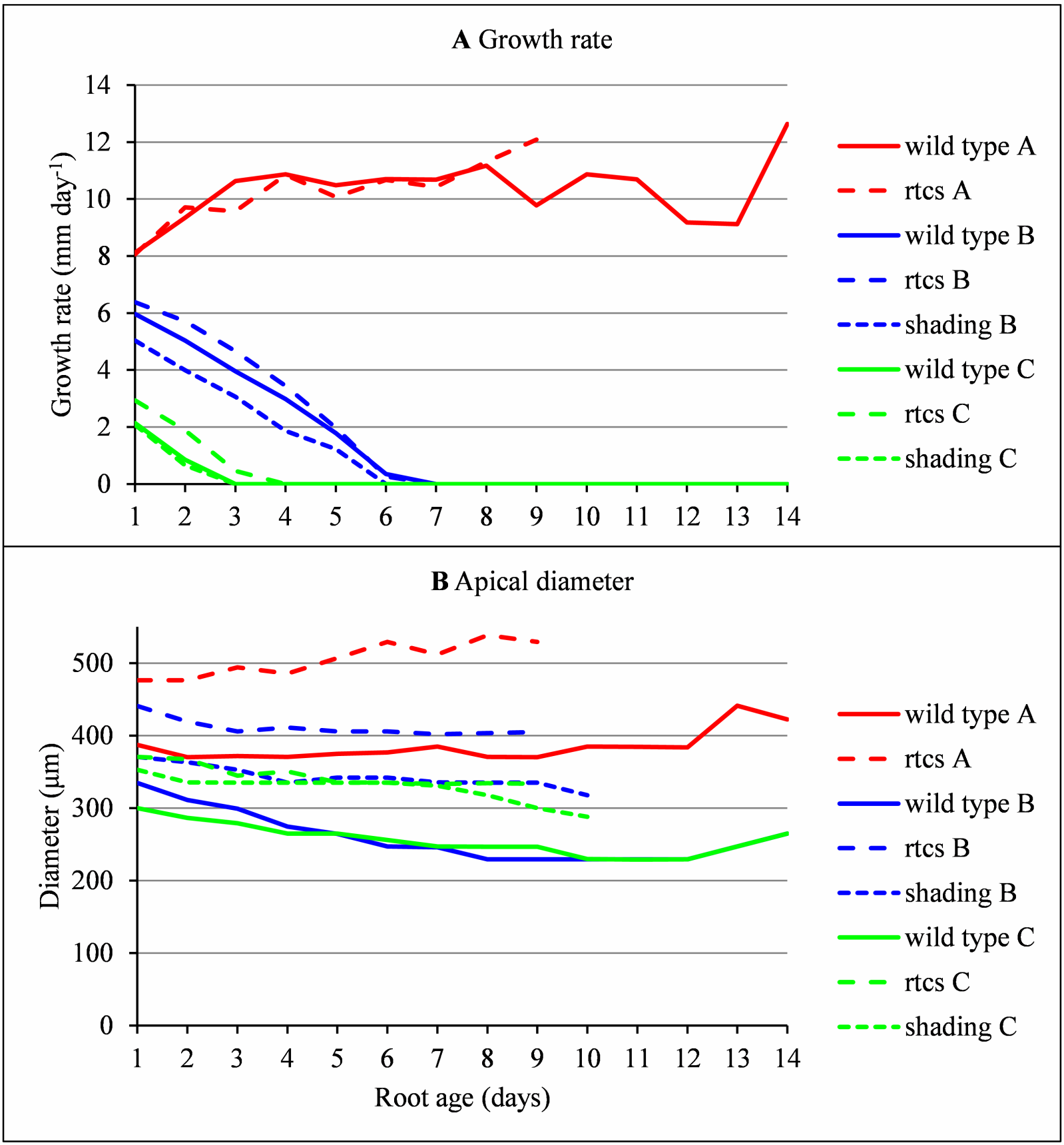

Figure 8. Daily median growth rates and apical diameters of lateral roots in wild-type, *rtcs* mutant and shaded maize.

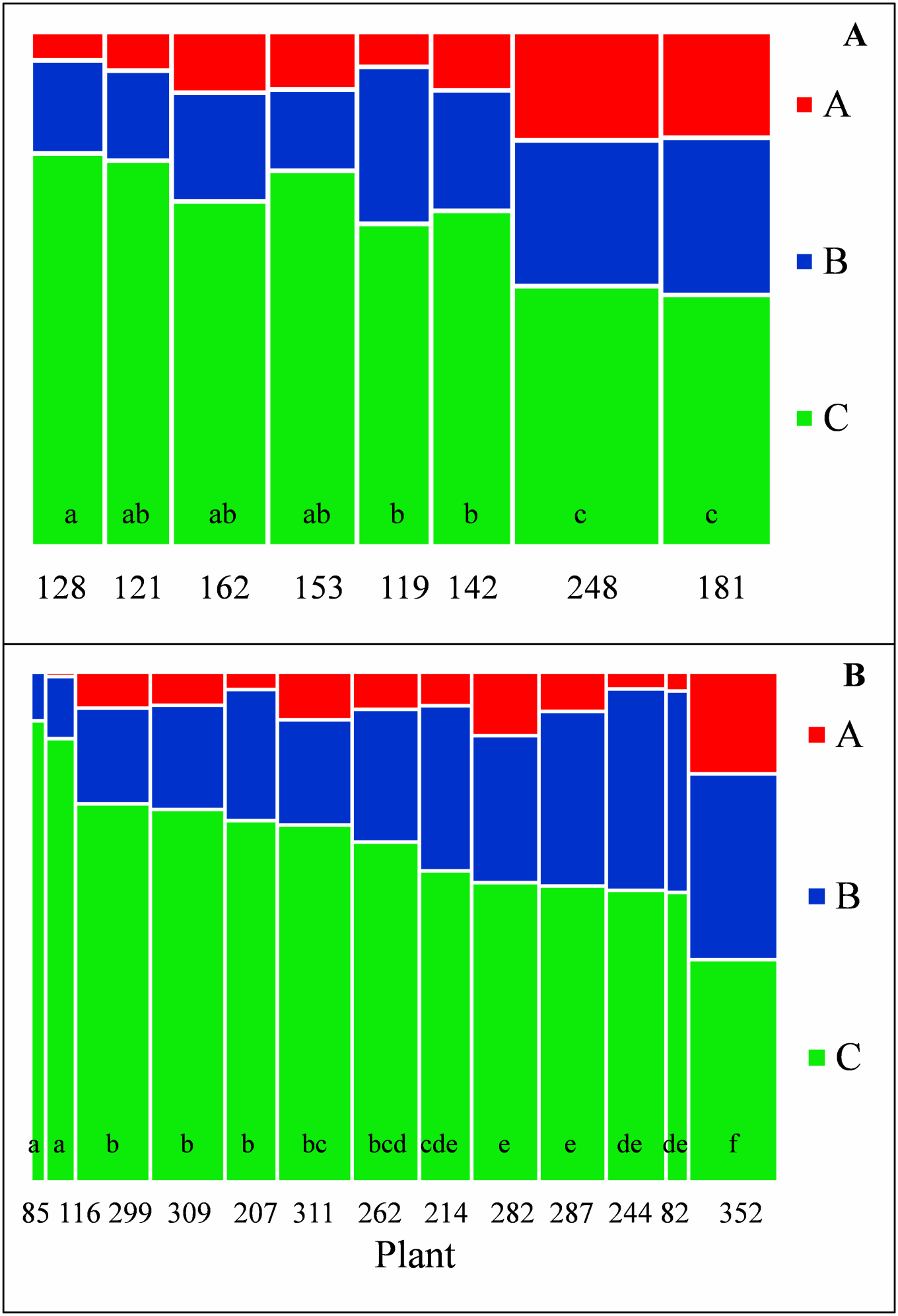

Figure 9. Proportions of lateral root types.

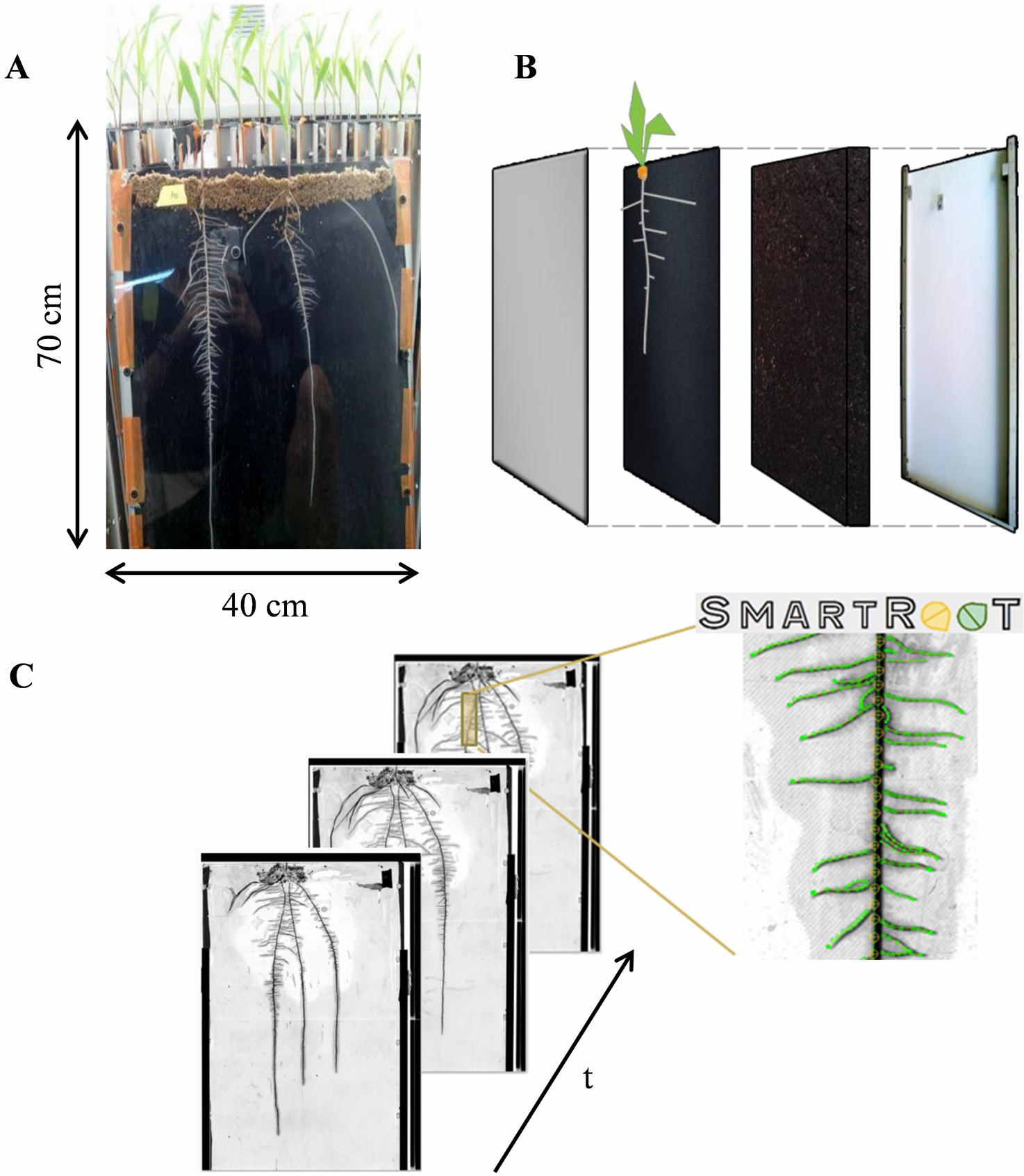

Figure 10. Rhizotron development and root system measurement.

Parsed Citations

Aguirrezabal LAN, Deleens E, Tardieu F (1994). Root elongation rate is accounted for by intercepted PPFD and source-sink relations in field and laboratory-grown sunflower. Plant, Cell Environ. 17: 443–450.
Pubmed: Author and Title
CrossRef: Author and Title
Google Scholar: Author Only Title Only Author and Title

Aschehoug ET, Callaway RM (2014). Morphological variability in tree root architecture indirectly affects coexistence among competitors in the understory. Ecology 95: 1731–1736.
Pubmed: Author and Title
CrossRef: Author and Title
Google Scholar: Author Only Title Only Author and Title

Atkinson JA, Wingen LU, Griffiths M, Pound MP, Gaju O, Foulkes MJ, Le Gouis J, Griffiths S, Bennett MJ, King J. (2015). Phenotyping pipeline reveals major seedling root growth QTL in hexaploid wheat. J. Exp. Bot. 66: 2283–2292.
Pubmed: Author and Title
CrossRef: Author and Title
Google Scholar: Author Only Title Only Author and Title

Bingham IJ, Stevenson EA (1993). Control of root growth: effects of carbohydrates on the extension, branching and rate of respiration of different fractions of wheat roots. Physiol. Plantarum 88: 149–158.
Pubmed: Author and Title
CrossRef: Author and Title
Google Scholar: Author Only Title Only Author and Title

Bishopp A, Lynch JP (2015). The hidden half of crop yields. Nat. Plants 1: 15117.
Pubmed: Author and Title
CrossRef: Author and Title
Google Scholar: Author Only Title Only Author and Title

Bühlmann P, Wyner AJ (1999). Variable length Markov chains. Ann. Stat. 27: 480–513.
Pubmed: Author and Title
CrossRef: Author and Title
Google Scholar: Author Only Title Only Author and Title

Coutts MP (1987). Developmental processes in tree root systems. Can. J. For. Res. 17: 761–767.
Pubmed: Author and Title
CrossRef: Author and Title
Google Scholar: Author Only Title Only Author and Title

Csiszár I, Talata Z (2006). Context tree estimation for not necessarily finite memory processes, Via BIC and MDL. IEEE Trans. Inf. Theory 52: 1007–1016.
Pubmed: Author and Title
CrossRef: Author and Title
Google Scholar: Author Only Title Only Author and Title

De Smet I, Signora L, Beeckman T, Inzé D, Foyer CH, Zhang H (2003). An abscisic acid-sensitive checkpoint in lateral root development of Arabidopsis. Plant J. 33: 543–555.
Pubmed: Author and Title
CrossRef: Author and Title
Google Scholar: Author Only Title Only Author and Title

Dhondt S, Wuyts N, Inzé D (2013). Cell to whole-plant phenotyping: The best is yet to come. Trends Plant Sci. 18: 1360–1385.
Pubmed: Author and Title
CrossRef: Author and Title
Google Scholar: Author Only Title Only Author and Title

Drew MC (1975). Comparison of the effects of a localized supply of phosphate, nitrate, ammonium and potassium on the growth of the seminal root sytem, and the shoot, in barley. New Phytol. 75: 479–490.
Pubmed: Author and Title
CrossRef: Author and Title
Google Scholar: Author Only Title Only Author and Title

Fahlgren N, Feldman M, Gehan MA, Wilson MS, Shyu C, Bryant DW, Hill ST, McEntee CJ, Warnasooriya SN, Kumar I, et al (2015a). A versatile phenotyping system and analytics platform reveals diverse temporal responses to water availability in Setaria. Mol. Plant 8: 1520–1535.
Pubmed: Author and Title
CrossRef: Author and Title
Google Scholar: Author Only Title Only Author and Title

Fahlgren N, Gehan MA, Baxter I (2015b). Lights, camera, action: high-throughput plant phenotyping is ready for a close-up. Curr. Opin. Plant Biol. 24: 93–99.
Pubmed: Author and Title
CrossRef: Author and Title

Google Scholar: Author Only Title Only Author and Title

Farrar JF, Jones CL (1986). Modification of respiration and carbohydrate status of barley roots by selective pruning. New Phytol. 102: 513–521.
Pubmed: Author and Title
CrossRef: Author and Title
Google Scholar: Author Only Title Only Author and Title

Forde BG (2009). Is it good noise? The role of developmental instability in the shaping of a root system. J. Exp. Bot. 60, 3989–4002.
Pubmed: Author and Title
CrossRef: Author and Title
Google Scholar: Author Only Title Only Author and Title

Freixes S, Thibaud M-C, Tardieu F, Muller B (2002). Root elongation and branching is related to local hexose concentration in Arabidopsis thaliana seedlings. Plant, Cell Environ. 25: 1357–1366.
Pubmed: Author and Title
CrossRef: Author and Title
Google Scholar: Author Only Title Only Author and Title

Gowda VRP, Henry A, Yamauchi A, Shashidhar HE, Serraj R (2011). Root biology and genetic improvement for drought avoidance in rice. Field Crops Res. 122: 1–13.
Pubmed: Author and Title
CrossRef: Author and Title
Google Scholar: Author Only Title Only Author and Title

Guédon Y (2003). Estimating hidden semi-Markov chains fom discrete sequences. J. Comput. Graph. Stat. 12: 604–639.
Pubmed: Author and Title
CrossRef: Author and Title
Google Scholar: Author Only Title Only Author and Title

Henry S, Divol F, Bettembourg M, Bureau C, Guiderdoni E, Périn C, Dievart A (2016). Immunoprofiling of rice root cortex reveals two cortical subdomains. Front. Plant Sci. 6: 1–9.
Pubmed: Author and Title
CrossRef: Author and Title
Google Scholar: Author Only Title Only Author and Title

Hetz W, Hochholdinger F, Schwall M, Feix G (1996). Isolation and characterization of rtcs, a maize mutant deficient in the formation of nodal roots. Plant J. 10: 845–857.
Pubmed: Author and Title
CrossRef: Author and Title
Google Scholar: Author Only Title Only Author and Title

Iyer-Pascuzzi, AS, Symonova O, Mileyko Y, Hao Y, Belcher H, Harer J, Weitz JS, Benfey PN (2010). Imaging and analysis platform for automatic phenotyping and trait ranking of plant root systems. Plant Physiol. 152: 1148–1157.
Pubmed: Author and Title
CrossRef: Author and Title
Google Scholar: Author Only Title Only Author and Title

Jordan MO, Harada J, Bruchou C, Yamazaki K (1993). Maize nodal root ramification: Absence of dormant primordia, root classification using histological parameters and consequences on sap conduction. Plant Soil 153: 125–143.
Pubmed: Author and Title
CrossRef: Author and Title
Google Scholar: Author Only Title Only Author and Title

Kuijken RCP, van Eeuwijk FA, Marcelis LFM, Bouwmeester HJ (2015). Root phenotyping: from component trait in the lab to breeding. J. Exp. Bot. 66: 5389–5401.
Pubmed: Author and Title
CrossRef: Author and Title
Google Scholar: Author Only Title Only Author and Title

Lavenus J, Goh T, Roberts I, Guyomarc'h S, Lucas M, De Smet I, Fukaki H, Beeckman T, Bennett M, Laplaze L (2013). Lateral root development in Arabidopsis: fifty shades of auxin. Trends Plant Sci., 18: 450–458.
Pubmed: Author and Title
CrossRef: Author and Title
Google Scholar: Author Only Title Only Author and Title

Lecompte F, Pagès L, Ozier-Lafontaine H (2005). Patterns of variability in the diameter of lateral roots in the banana root system. New Phytol. 167: 841–850.
Pubmed: Author and Title
CrossRef: Author and Title
Google Scholar: Author Only Title Only Author and Title

Lièvre M, Granier C, Guédon Y (2016). Identifying developmental phases in the Arabidopsis thaliana rosette using integrative segmentation models. New Phytol. 210: 1466–1478.
Pubmed: Author and Title
CrossRef: Author and Title

Google Scholar: Author Only Title Only Author and Title

Lobet G, Pagès L, Draye X (2011). A novel image-analysis toolbox enabling quantitative analysis of root system architecture. Plant Physiol. 157: 29–39.
Pubmed: Author and Title
CrossRef: Author and Title
Google Scholar: Author Only Title Only Author and Title

Lynch JP. (2018) Rightsizing root phenotypes for drought resistance. J. Exp. Bot. in press.
Pubmed: Author and Title
CrossRef: Author and Title
Google Scholar: Author Only Title Only Author and Title

MacLeod RD (1990). Lateral root primordium inception in Zea mays L. Environ. Exp. Bot. 30: 225–234.
Pubmed: Author and Title
CrossRef: Author and Title
Google Scholar: Author Only Title Only Author and Title

Maiti RK, Bidinger FR (1981). Growth and development of the pearl millet plant. ICRISAT Res. Bull. 6.
Pubmed: Author and Title
CrossRef: Author and Title
Google Scholar: Author Only Title Only Author and Title

Malamy JE (2005). Intrinsic and environmental response pathways that regulate root system architecture. Plant, Cell Environ. 28: 67–77.
Pubmed: Author and Title
CrossRef: Author and Title
Google Scholar: Author Only Title Only Author and Title

Moreno-Ortega B, Fort G, Muller B, Guédon Y (2017). Identifying developmental zones in maize lateral root cell length profiles using multiple change-point models. Front. Plant Sci. 8: 1750.
Pubmed: Author and Title
CrossRef: Author and Title
Google Scholar: Author Only Title Only Author and Title

Muller B, Stosser M, Tardieu F (1998). Spatial distributions of tissue expansion and cell division rates are related to irradiance and to sugar content in the growing zone of maize roots. Plant, Cell Environ. 21: 149–158.
Pubmed: Author and Title
CrossRef: Author and Title
Google Scholar: Author Only Title Only Author and Title

Nestler J, Keyes SD, Wissuwa M. (2016). Root hair formation in rice (Oryza sativa L.) differs between root types and is altered in artificial growth conditions. J Exp. Bot. 67: 3699–3708.
Pubmed: Author and Title
CrossRef: Author and Title
Google Scholar: Author Only Title Only Author and Title

Neufeld HS, Durall DM, Rich PM, Tingey DT (1989). A rootbox for quantitative observations on intact entire root systems. Plant Soil 117: 295–298.
Pubmed: Author and Title
CrossRef: Author and Title
Google Scholar: Author Only Title Only Author and Title

Pagès L (1995). Growth patterns of the lateral roots of young oak (Quercus robur) tree seedlings Relationship with apical diameter. New Phytol. 130: 503–509.
Pubmed: Author and Title
CrossRef: Author and Title
Google Scholar: Author Only Title Only Author and Title

Pagès L (2011). Links between root developmental traits and foraging performance. Plant. Cell Environ. 34 : 1749–1760.
Pubmed: Author and Title
CrossRef: Author and Title
Google Scholar: Author Only Title Only Author and Title

Passot S, Gnacko F, Moukouanga D, Lucas M, Guyomarc'h S, Moreno Ortega B, Atkinson JA, Belko MN, Bennett MJ, Gantet P et al (2016). Characterization of pearl millet root architecture and anatomy reveals three types of lateral roots. Front. Plant Sci. 7: 1–11.
Pubmed: Author and Title
CrossRef: Author and Title
Google Scholar: Author Only Title Only Author and Title

Rebouillat J, Dievart A, Verdeil JL, Escoute J, Giese G, Breitler JC, Gantet P, Espeout S, Guiderdoni E, Périn C (2009). Molecular genetics of rice root development. Rice 2: 15–34.
Pubmed: Author and Title
CrossRef: Author and Title
Google Scholar: Author Only Title Only Author and Title

Ron D, Singer Y, Tishby N (1997). The power of amnesia: Learning probabilistic automata with variable memory length. Mach. Learn. 25:

117–149.
Pubmed: Author and Title
CrossRef: Author and Title
Google Scholar: Author Only Title Only Author and Title

Saengwilai P, Tian X, Lynch JP (2014). Low crown root number enhances nitrogen acquisition from low-nitrogen soils in maize. Plant Physiol. 166: 581–589.
Pubmed: Author and Title
CrossRef: Author and Title
Google Scholar: Author Only Title Only Author and Title

Taramino G, Sauer M, Stauffer JL, Multani D, Niu X., Sakai H, Hochholdinger F (2007). The maize (Zea mays L.) RTCS gene encodes a LOB domain protein that is a key regulator of embryonic seminal and post-embryonic shoot-borne root initiation. Plant J. 50: 649659.
Pubmed: Author and Title
CrossRef: Author and Title
Google Scholar: Author Only Title Only Author and Title

Thaler P, Pagès L (1996). Root apical diameter and root elongation rate of rubber seedlings (Hevea brasiliensis) show parallel responses to photoassimilate availability. Physiol. Plant. 97: 365–371.
Pubmed: Author and Title
CrossRef: Author and Title
Google Scholar: Author Only Title Only Author and Title

Topp CN, Iyer-Pascuzzi AS, Anderson JT, Lee C-R, Zurek PR, Symonova O, Zheng Y, Bucksch A, Mileyko Y, Galkovskyi T, et al (2013). 3D phenotyping and quantitative trait locus mapping identify core regions of the rice genome controlling root architecture. Proc. Natl. Acad. Sci. U. S. A. 110: E1695–704.
Pubmed: Author and Title
CrossRef: Author and Title
Google Scholar: Author Only Title Only Author and Title

Varney GT, Canny MJ, Wang XL, McCully ME (1991). The branch roots of Zea. I. First order branches, their number, sizes and division into classes. Ann. Bot. 67: 357–364.
Pubmed: Author and Title
CrossRef: Author and Title
Google Scholar: Author Only Title Only Author and Title

Varney GT, McCully, ME (1991). The branch roots of Zea. II. Developmental loss of the apical meristem in field-grown roots. New Phytol. 118: 535–546.
Pubmed: Author and Title
CrossRef: Author and Title
Google Scholar: Author Only Title Only Author and Title

Vejchasarn P, Lynch JP, Brown KM. (2016). Genetic variability in phosphorus responses of rice root phenotypes. Rice 9: 29.
Pubmed: Author and Title
CrossRef: Author and Title
Google Scholar: Author Only Title Only Author and Title

Wang XL, McCully ME, Canny MJ. (1994). The branch roots of Zea. IV. The maturation and openness of xylem conduits in first-order branches of soil-grown roots. New Phytol. 126: 21–29.
Pubmed: Author and Title
CrossRef: Author and Title
Google Scholar: Author Only Title Only Author and Title

Watt M, Magee LJ, McCully, ME (2008). Types, structure and potential for axial water flow in the deepest roots of field-grown cereals. New Phytol. 178: 135–146.
Pubmed: Author and Title
CrossRef: Author and Title
Google Scholar: Author Only Title Only Author and Title

Williamson LC, Ribrioux SPCP, Fitter AH, Leyser HMO (2001). Phosphate Availability Regulates Root System Architecture in Arabidopsis. Plant Physiol. 126: 875–882.
Pubmed: Author and Title
CrossRef: Author and Title
Google Scholar: Author Only Title Only Author and Title

Wu Q, Pagès L, Wu J (2016). Relationships between root diameter, root length and root branching along lateral roots in adult, field-grown maize. Ann. Bot. 117:379–390.
Pubmed: Author and Title
CrossRef: Author and Title
Google Scholar: Author Only Title Only Author and Title

Zhu J, Brown KM, Lynch JP (2010). Root cortical aerenchyma improves the drought tolerance of maize (Zea mays L.). Plant, Cell Environ. 33: 740–749.
Pubmed: Author and Title
CrossRef: Author and Title

Google Scholar: Author Only Title Only Author and Title